

**Reliability Study of Hermetic Packages for
High-Frequency Applications:
Characterization of Microwave/Millimeterwave Packages**

Report Number: 035151-F-1

August 1998

**Linda P.B. Katehi
Donghoon Chen
Jong-Gwan Yook
George E. Ponchak**

35151-1-F = RL-2493

**Reliability Study of Hermetic Packages for
High-Frequency Applications:
Characterization of Microwave/Millimeterwave Packages**

Abstract

This report presents the electromagnetic characteristics of vias to microwave/millimeterwave circuits in packages and the suppression of higher order modes of package using vias. In the former case, five different structures are studied using finite element method (FEM) as the location of vias is moved from the circuits; microstrip/strip through-line with arrays of vias parallel to the microstrip/stripline, microstrip/strip through-line with twelve vias parallel to the microstrip/stripline, strip through-line with six vias vertical to the stripline. Two cavity structures are simulated in the latter case using FEM as distance between vias is changed; cavity with open striplines and vias located between the striplines. Computed scattering parameters and quantitative data are shown to visualize the cavity mode suppression. Design rules for the suppression of cavity modes and the package design are presented in this report.

I. INTRODUCTION

As there are rapid advances of monolithic microwave integrated circuit (MMIC) technology, the importance of the efficient packaging of microwave/millimeter-wave circuits is emphasized. As a result, there have been efforts to develop the advanced packaging technology to make the package with less weight, improved performance, increased density and productivity. The package for microwave/millimeter-wave circuits itself must have a series of functions to provide the circuits contained within them with electrical/thermal interference and mechanical/environment protection. While the package provides the circuits with those beneficial functions, it also degrades the performance of the circuit components that it contains. Therefore, in order to avoid maleficent effects of the package on the circuits, the package should have minimum insertion and reflection losses associated with both the interior of the package and the input/output port. Furthermore, the package should not have the package-generated resonances and related effects. As a result of all these requirements and the need to develop the advanced packaging technology, the design engineers need sophisticated design tools and careful design schemes for the successful package design and the realization of the advanced packages. Currently, however, most of available commercial design tools can not analyze many package effects such as resonances[2]. Therefore it is important to give design rules and analyze many package effects for designing such high performance/high frequency packages. In this report, the electromagnetic (EM) effect of vias on microstrip/stripline is studied for different locations of vias and design rules are presented. Furthermore, the suppression of higher order mode in the package is investigated for the cavity with stripline by adjusting distance between vias. All the simulations are accomplished by a parallelized three-dimensional (3-D) finite element method (FEM). The IBM SP2 parallel computer with distributed memory and optimization is used for the simulation. The performance of the

parallelized 3-D FEM program is near linearly improved with respect to the number of processes that are used, because of the independent nature of the problem in the frequency domain[3].

II. NUMERICAL RESULTS AND DISCUSSIONS

In this section, seven different structures are simulated for the characterization of microwave/millimeter-wave packages; microstrip/stripline with arrays of vias parallel to the microstrip/stripline, microstrip/stripline with twelve vias parallel to the microstrip/stripline, stripline with six vias vertical to the stripline, cavity with open striplines and vias located between the striplines, and cavity with bended stripline and vias parallel to the bended stripline.

In the first five cases, artificial absorber is used around the structure using lossy isotropic dielectrics for the simulation of open structure. The goal of these cases is to study the EM characteristics of vias to MMIC in terms of distance between the circuit and vias and distance between vias. Average scattering parameters and average radiation loss are shown in the results for the first five cases, because they are nearly uniform over the frequency.

In the last two cases, the higher order mode suppression is studied by placing vias in the package and changing gaps between vias.

II-A. MICROSTIP THROUGH-LINE WITH ARRAYS OF VIAS PARALLEL TO THE MICROSTRIP

As shown in Fig. 1, Fig. 2 and Fig. 3, arrays of vias are placed along the center conductor of microstrip through-line with the distance of ΔS . The separation between vias is designated as Δh and two different separation cases are studied in this structure; $\Delta h = 1.6 h$ and $6 h$. The distance between the center conductor of the microstrip-line and the vias, ΔS , is varied from $1 h$ to $4 h$. Other parameters used in this structure are $D_v = 0.25$ mm (diameter of via), $\epsilon_r = 5.3$ (dielectric constant of substrate) and $h = 0.25$ mm (thickness of substrate).

Because of the nearly uniform values of scattering parameter over the frequency, average scattering parameters are calculated for different Δh and ΔS (see Fig. 4 and Fig. 5). The results show that insertion loss and radiation loss become high when vias are close to the center conductor of microstrip. It is also noted that scattering parameter and radiation loss are improved as gaps between vias are reduced, because dense via wall shields EM energy leakage through vias better than sparse via wall. Return loss is less than -25 dB over all ΔS and Δh . For $\Delta h = 6$ h, insertion loss changes from -0.38 dB to -0.127 dB and radiation loss drops from -11.1 dB to -15.67 dB as arrays of vias are moved from $\Delta S = 1$ h to 4 h. Similar trend can be observed in radiation loss and insertion loss for $\Delta h = 1.6$ h. When ΔS is changed from 1 h to 4 h for $\Delta h = 1.6$ h, radiation loss becomes -17.65 dB from -12 dB and insertion loss is improved by -0.11 dB from -0.289 dB. Field distribution for $\Delta h = 6$ h is shown in Fig. 6 and $\Delta h = 1.6$ h in Fig. 7.

II-B. MICROSTRIP THROUGH-LINE WITH TWELVE VIAS PARALLEL TO THE MICROSTRIP

For the purpose of extensive study of case II-A, we take twelve vias located along microstrip through-line from the structure of case II-A. So all the parameters in the structure are same with those of the case II-A except Δh is 1.6 h. The schematic diagram, crosssection, and top view of the circuit are shown in Fig. 8, Fig. 9 and Fig. 10.

As it can be observed in Fig. 11 and Fig. 12, there is much variation in average scattering parameters and radiation loss when ΔS is changed from 1 h to 2 h while there are small variations for the rest cases of ΔS . We believe that this phenomenon is due to the small number of vias. Insertion loss for $\Delta S = 1$ h is -0.57 dB and it remains between -0.24 dB and -0.15 dB when the via is moved to 2 h or further from the microstrip. Insertion loss is -25 dB for $\Delta S = 1$ h, but it stays under -33 dB for the rest of ΔS . Smiliar trends can be observed in radiation loss. Radiation loss is -9.47 dB when vias are located at 1 h from the microstrip and stays between

-12.8 dB and -14.8 dB after the vias are moved to $2h$ or further. Field distribution for this structure is shown in Fig. 13.

II-C. STRIPLINE WITH ARRAYS OF VIAS PARALLEL TO THE STRIPLINE

Stripline is studied with the same situation as the microstrip case II-A. Arrays of vias are again placed along stripline with the distance of ΔS from the stripline and with the separation of Δh between vias. The height of stripline, H , is 0.5 mm and other parameters are exactly same with those of the microstrip through-line case II-A. The schematic diagram, cross-section, and top view of this structure are shown in Fig. 14, Fig. 15 and Fig. 16.

Similar to microstrip case II-A, stripline with dense vias has better EM performance for vias than the one with sparse vias, because dense via wall shows better shielding effect on the EM field than sparse vias as we can see in (Fig. 19, Fig. 20. As shown in Fig. 17 and Fig. 18, insertion loss is better than -0.1 dB and radiation loss is less than -17 dB for $\Delta h = 1.3 h$ over all ΔS while the lowest insertion loss is -0.187 dB and the largest radiation loss is -14.07 dB for $\Delta h = 5.2 h$ over all ΔS . Return losses for both Δh are less than -27 dB over all ΔS . The variation of average scattering parameter and radiation loss with respect to ΔS is smaller than the microstrip case II-A. It is noted that stripline shows better electromagnetic performance for vias than microstrip case II-A. One can visually understand this phenomenon by comparing field distribution of microstrip (Fig. 6, Fig. 7) and stripline (Fig. 19, Fig. 20. As we can observe in the field distributions, most of EM field from stripline is shield by vias in this case. Therefore stripline shows lower radiation loss than microstrip. Stripline also has better insertion loss and return loss for vias than microstrip.

II-D. STRIPLINE WITH TWELVE VIAS PARALLEL TO THE STRIPLINE

As one can see in Fig. 21, Fig. 22 and Fig. 23, twelve vias are placed in stripline and calculated average scattering parameter (see Fig. 24, Fig. 25). The separation of vias, Δh , is $1.3 h$ and the height of stripline, H , is 0.5 mm . Other parameters, for example ΔS and ϵ_r , are equal to those of microstrip through-line case II-A.

Scattering parameters and radiation loss for $\Delta S = 3 h$ is slightly poorer than those for $\Delta S = 2 h$ due to, we believe, the numerical error. Generally, it is understood that vias far from the center conductor of stripline have less interactions with the EM field generated by stripline than vias close to the center conductor of stripline. Compared to the results for the case of microstrip through-line with twelve vias, insertion loss and radiation loss for this case are similar to those of microstrip case II-B. Return loss is, however, higher than the one for the microstrip case II-B and it is less than -24 dB over all ΔS . Insertion loss is -0.5 dB and radiation loss is -9.8 dB for $\Delta S = 1 h$. When vias are moved to $\Delta S = 4 h$, insertion loss becomes -0.18 dB and radiation loss downs to -14 dB . Field distribution at 35 GHz is shown in Fig. 26.

II-E. STRIP THROUGH-LINE WITH SIX VIAS VERTICAL TO THE STRIPLINE

In this case, we placed six vias vertical to the center conductor of stripline and studied the EM effect of vias on stripline in terms of ΔS and Δh by calculating average scattering parameters and radiation loss on the stripline. All of the parameters are identical with those of the stripline case II-D. The schematic diagram, cross-section, and top view of the circuit are shown in Fig. 27, Fig. 28 and Fig. 29.

In the case of II-A and II-C where vias are located parallel to the microstrip/stripline, insertion loss and radiation loss are decreased as Δh is reduced. But when vias are placed vertically to stripline in this case, insertion loss and radiation loss are increased as Δh is reduced. This result can be understood by investigating the EM field distribution over the vertically located

vias. In this structure, most of the EM field is concentrated on the center conductor of stripline and decayed very fast from the center conductor of stripline. Thus when the gap between vias, Δh , is reduced, vias are close to the center conductor of stripline. As a result, vias have more interaction with EM field near stripline. One can visually understand this phenomenon with field distribution for each Δh shown in Fig. 32 and Fig. 33. Return losses for all Δh values are lower than -20 dB. When vias are moved from $\Delta S = 1 h$ to $4 h$, insertion loss changes from -0.32 dB to -0.22 dB for $\Delta h = 5.2 h$ and from -0.5 dB to -0.28 dB for $\Delta h = 1.3 h$. Radiation loss for $\Delta h = 5.2 h$ downs from -12.11 dB to -13.88 dB while the one for $\Delta h = 1.3 h$ is decreased from -10 dB to -12.6 dB over all ΔS .

II-F. CAVITY WITH OPEN STRIPLINES AND WITH VIAS LOCATED BETWEEN THE STRIPLINES

Two isolated open striplines are placed in cavity and vias are located between the striplines. The schematic diagram and top view (at $h = 0.25$ mm) of the structure is shown in Fig. 34 and Fig. 35. Parameters used in this structure are $D_v = 0.25$ mm (diameter of via), $h = 0.25$ mm (height of the center conductor of stripline), $a = 2.13$ mm (width of the cavity), $d = 7.2$ mm (distance between center conductors of striplines), $H = 0.5$ mm (height of the cavity) and $\epsilon_r = 5.3$ (dielectric constant). Distance between vias, Δh , is changed from $57.228 h$ to $13.932 h$.

For the simulation of this structure, only one of the two striplines is excited. In order to visualize the suppression of higher order mode in quantitative way, the field ratio, maximum magnitude of total electric field on the unexcited stripline divided by the one on the excited stripline, is calculated (see Fig. 36, Fig. 37 and Fig. 38).

As it can be observed in Fig. 36, higher order modes are generated from cutoff frequency of the cavity's dominant mode when there are no vias. As Δh is gradually reduced (vias are added), the cutoff frequency shifts to the higher frequency and the number of resonating frequency is

reduced. When Δh is smaller than 6.716 h, the ratio is less than -50dB (see Fig. 38). This observation indicates that unwanted higher order modes can be suppressed by placing vias with separation of $0.394 \lambda_c$ for any type of the cavity, where λ_c is the cutoff wavelength of dominant mode in the cavity. Quantative data are shown in Fig. 39, Fig. 40, and Fig. 41. As is shown in Fig. 39, there are no higher order modes under cutoff frequency when the gap between vias is 57.228 h. Once operating frequency is above cutoff frequency, there exist higher order modes above cutoff frequency when $\Delta h = 57.228$ h (see Fig. 40). Fig. 41 shows the suppression of higher order mode at the operating frequency above cutoff frequency by reducing the distance between vias to 6.716 h.

II-G. CAVITY WITH BENDED STRIP THROUGH-LINE AND WITH VIAS PARALLEL TO THE BENDED STRIPLINE

As was the case II-F, the suppression of higher order modes is explored for different type of cavity. Bended strip through-line is placed in cavity and vias are located along the bended stripline (see Fig. 42 and Fig. 43). The dimensions and ϵ_r are same with those of the previous case II-F except $a = 3.13$ mm and Δh . Scattering parameters for different Δh are calculated and shown in Fig. 44 and Fig. 45.

When there are no vias, as shown in Fig. 44, scattering parameters are degraded from cutoff frequency because of higher order modes. But scattering parameters are gradually stabilized as Δh is reduced, which means higher order modes are successfully suppressed when Δh is 6.2 h or smaller (see Fig. 45). Fig. 46, Fig. 47, and Fig. 48 show quantative data for this case. Fig. 46 and Fig. 47 show the absence of higher order modes under cutoff frequency and the existence of higher order modes above cutoff frequency for $\Delta h = 56.76$. The suppression of higher order modes by reducing Δh to 6.2 h is shown in Fig. 48. This result confirms the conclusion of the

previous case II-F that vias can be used to suppress unwanted resonance in any type of cavity.

III. DESIGN RULES

III-A. MICROSTRIP THROUGH-LINE WITH THE ARRAY OF VIAS PARALLEL TO THE MICROSTRIP

III-A-1. THE CASE OF $\Delta H = 6 H$

When ΔS is changed from 1 h to 3h, scattering parameters and radiation loss of microstrip are linearly changed with respect to ΔS . Insertion loss of microstrip has -0.24 dB variation and radiation loss of microstrip is varied from -11.1 dB to -15.17 dB by vias. Similarly, return loss of microstrip is decreased from -24.4 dB to -32.86 dB.

Vias located at 3 h and 4 h from microstrip show identical EM characteristics on microstrip, thus vias can be placed either at 3 h or 4 h from microstrip with same EM affections from vias. Radiation loss of microstrip is -15 dB and return loss -32 dB when ΔS is 3 h and 4 h. Insertion loss of microstrip is -0.14 dB for $\Delta S = 3$ h and 4 h..

III-A-2. THE CASE OF $\Delta H = 1.6 H$

Array of vias with $\Delta h = 1.6$ h has more shielding effect for EM field from microstrip than the one with $\Delta h = 6$ h. Scattering parameters and radiation loss of microstrip are better than previous case but the trend with respect to ΔS is same. When vias are moved from 1 h to 3 h, radiation loss of microstrip is decreased linearly from -12 dB to -16 dB and variation of insertion loss is -0.18 dB. Return loss of microstrip is, however, -30 dB for $\Delta S = 1$ h and -35 dB for the rest of ΔS .

Placing vias either 3 h or 4 h from microstrip give microstrip nearly same EM affection. Variations of insertion loss is only -1.32 dB and radiation loss -0.03 dB.

III-B. MICROSTRIP THROUGH-LINE WITH THE TWELVE VIAS PARALLEL TO THE MICROSTRIP

In this case radiation loss and insertion loss of microstrip are clearly affected by vias when ΔS is 1 h compared to the rest of ΔS . Vias located at 1 h from microstrip affect return loss of microstrip to be -25 dB and radiation loss -9.47 dB. Variation of insertion loss is -0.33 dB when ΔS is changed from 1 h to 2 h. When vias are placed between 2h and 4h from microstrip, variation of insertion loss of microstrip is only -0.09 dB and radiation loss of microstrip is between -12.8 dB and -14.8 dB. Return loss of microstrip is less than -33 dB when ΔS is between 2 h and 4 h. Therefore vias can be placed at between 2 h and 4 h from microstrip without giving much variations of EM performance of microstrip.

III-C. STRIP THROUGH-LINE WITH THE ARRAY OF VIAS PARALLEL TO THE STRIPLINE

In stripline case scattering parameters and radiation loss do not varies as much as micristrip case for both Δh with respect to ΔS . The EM performance of stripline with dense vias is better than the one with sparse vias.

III-C-1. THE CASE OF $\Delta H = 5.2 H$

Radiation loss and insertion loss are linearly changed as ΔS is increased in this case. Vias can be placed at $\Delta S = 1$ h from the stripline with tolerance of -0.187 dB for insertion loss and -14 dB for radiation loss. When ΔS is varied from 1 h to 4 h, vias affect radiation loss of stripline to decrease from -14 dB to -17.12 dB. Variation of insertion loss of stripline is -0.096 dB. Return loss of stripline is less than -27 dB over all ΔS .

III-C-2. THE CASE OF $\Delta H = 1.3 H$

For $\Delta h = 1.3$ h vias can be placed at either $\Delta S = 1$ h or 2 h with same EM effect on insertion loss and radiation loss of stripline. Variation of insertion loss of stripline is only -0.004 dB and radiation loss of stripline is -17 dB when ΔS is 1 h or 2 h. Similarly, locating vias at $\Delta S = 3$ h and 4h give equal EM influence on stripline. Insertion loss of stripline is -0.05 dB and

radiation loss of stripline is -20 dB for $\Delta S = 3$ h and 4 h. Return loss of stripline is less than -28 dB over all ΔS .

III-D. STRIPLINE WITH TWELVE VIAS PARALLEL TO THE STRIPLINE

When vias are separated by 1 h from stripline, radiation loss and scattering parameters of stripline are much affected by vias than other ΔS values. Vias placed at $\Delta S = 1$ h influence radiation loss of stripline to be -9.8 dB and return loss -24.89 dB. Insertion loss of stripline is -0.5 dB for $\Delta S = 1$ h. The existence of vias between 2 h and 4 h from stripline do not change the performance of stripline much. Return loss of stripline is -26 dB and radiation loss is changed between -13.2 dB and -14.19 dB. The variation of insertion loss is only -0.096 dB when ΔS is between 2 h and 4 h.

III-E. STRIPLINE WITH SIX VIAS VERTICAL TO THE STRIPLINE

When package has vias vertical to MMIC, vias with small Δh show more EM interaction than vias with large Δh because more vias are exposed to strong EM field concentrated on the circuits. As a result, stripline with vias of $\Delta h = 5.2$ h shows better EM performance than the one with vias of $\Delta h = 1.3$ h. Therefore it is desirable to have large separation between vias as possible.

III-E-1. THE CASE OF $\Delta H = 1.3$ H

Return loss of stripline over all Δ is almost uniform in this case and it remains between -22 dB and -24 dB. Radiation loss of stripline is decreased and insertion loss of stripline is linearly changed with respect to ΔS for the values of ΔS between 1 h and 3 h. Radiation loss of stripline is decreased from -10 dB to -12.56 as ΔS is varied from 1 h to 3 h. Vias at 3 h and 4 h show same EM characteristics on stripline. As a result, vias can be placed either 3 h or 4 h without much

variations to scattering parameters and radiation loss of stripline. Radiation loss of stripline is -12.56 dB when via is located at 3 h or 4 h from stripline.

III-E-2. THE CASE OF $\Delta H = 5.2 H$

In this case stripline feels same EM influence by vias located at 1 h and 2 h from the stripline. Vias can be placed at 1h and 2 h from stripline with radiation loss of stripline by -12 dB and insertion loss of stripline by -0.31 dB. Return loss of stripline is -21 dB for $\Delta S = 1 h$ and 2 h. Similarly, vias at 3 h and 4 h show same EM influence on stripline. Radiation loss of stripline is -13.7 dB and return loss is -22 dB when vias is placed at 3 h and 4 h from the stripline. Insertion loss of stripline is -0.22 dB with vias located at 3 h and 4 h from stripline. Therefore we can place vias at either 1 h or 2 h from stripline with same EM influence on the stripline. Similarly, vias can be located at either 3 h or 4 h from stripline for same reason.

III-F. CAVITY WITH OPEN STRIPLINES WITH VIAS LOCATED BETWEEN THE STRIPLINES

When there are open striplines in package, cavity modes can be suppressed by placing vias between the striplines. Distance between vias, Δh , should be less than $0.394 \lambda_c$ in order to suppress cavity mode under -50dB, where λ_c is the cutoff wavelength of dominant mode in the cavity.

III-G. CAVITY WITH BENDED STRIP THROUGH-LINE AND WITH VIAS PARALLEL TO THE BENDED STRIPLINE

When package has a bended stripline, cavity modes can be suppressed by placing vias along the striplines. For the cavity modes suppression distance between vias, Δh , should not larger than $0.248 \lambda_c$, where λ_c is the cutoff wavelength of dominant mode in the cavity.

IV. CONCLUSION

In this report, the electromagnetic characteristics of vias to microwave/millimeter-wave circuits in packages are studied using finite element method (FEM). The results show that vias have more electromagnetic interactions when they are closer to the microwave/millimeter-wave circuits. As a result, vias close to MMIC give more EM influence on the circuits. The results also show that stipline is less sensitive to vias than microstrip.

We further investigated the suppression of cavity mode by placing vias in cavity and changing distance between vias. The results show that unwanted cavity mode in packages can be suppressed by placing vias which is separated by the distance shown in this report. With the results produced in this report, we could make design rules for the suppression of cavity mode and package design.

ACKNOWLEDGMENT

This work is supported by NASA Lewis Research Center. The authors would like to acknowledge the use of parallel computers from the University of Michigan Center for Parallel Computing (CPC).

References

- [1] Jong-Gwan Yook, Linda P. B. Katehi, Rainee N. Simons, and Kurt A. Shalkhauser "The Experimental and Theoretical Study of Parasitic Leakage/Resonance in a K/KA-Band MMIC Package," *IEEE Trans. Microwave Theory Tech.*, pp.2403-2410, Dec. 1996.
- [2] Thomas A. Midfort, John J. Wooldridge, and Rich L. Sturdivant "The Evolution of Packages for Monolithic Microwave and Millimeter-Wave Circuits," *IEEE Trans. Microwave Theory Tech.*, pp.983-991, Sep. 1995.

- [3] Jong-Gwan Yook and Linda P. B. Katehi “Characterization of MMIC’s packages using a parallelized 3-D FEM code,” *1996 ACES Symp. Proc.*, Monterey, CA

List of Figures

1	Schematic diagram of the microstrip case II-A.	17
2	Cross section view of the microstrip case II-A.	17
3	Top view of the microstrip case II-A.	18
4	Computed return loss and rad. loss for the microstrip case II-A.	19
5	Computed insertion loss for the microstrip case II-A.	19
6	Field distribution for the microstrip case II-A at 25GHz ($\Delta h = 6 h$).	20
7	Field distribution for the microstrip case II-A at 25GHz ($\Delta h = 1.6 h$).	20
8	Schematic diagram of the microstrip case II-B.	21
9	Cross section view of the microstrip case II-B.	21
10	Top view of the microstrip case II-B.	22
11	Computed return loss and rad. loss for the microstrip case II-B.	23
12	Computed insertion loss for the microstrip case II-B.	23
13	Field distribution for the microstrip case II-A at 25GHz ($\Delta h = 1.6 h$).	24
14	Schematic diagram of the stripline case II-C.	25
15	Cross section view of the stripline case II-C.	25
16	Top view of the stripline case II-C at $h = 0.25mm$	26
17	Computed return loss and rad. loss for the stripline case II-C.	27
18	Computed insertion loss for the stripline case II-C.	27
19	Field distribution of the stripline case II-C at 25GHz. ($\Delta h = 5.2 h$)	28
20	Field distribution of the stripline case II-C at 25GHz. ($\Delta h = 1.3 h$)	28
21	Schematic diagram of the stripline case II-D.	29
22	Cross section view of the stripline case II-D.	29
23	Top view of the stripline case II-D at $h = 0.25mm$	30
24	Computed return loss and rad. loss for the stripline case II-D.	31
25	Computed insertion loss for the stripline case II-D.	31
26	Field distribution of the stripline case II-D at 35GHz. ($\Delta h = 1.3 h$)	32
27	Schematic diagram of the stripline case II-E.	33
28	Cross section view the stripline case II-E.	33
29	Top view of the stripline case II-E at $h = 0.25mm$	34
30	Computed return loss and rad. loss for the stripline case II-E.	35
31	Computed insertion loss for the stripline case II-E.	35
32	Field distribution of the stripline case II-E at 28GHz. ($\Delta h = 5.2 h$)	36
33	Field distribution of the stripline case II-E at 28GHz. ($\Delta h = 1.3 h$)	36
34	Schematic diagram of the cavity with open striplines case II-F.	37
35	Top view of the cavity with open striplines case II-F at $h = 0.25mm$	38
36	Ratio of maximum field value for the cavity with open striplines case II-F.	39
37	Ratio of maximum field value for the cavity with open striplines case II-F.	39
38	Ratio of maximum field value for the cavity with open striplines case II-F.	40

39	Field distribution for the cavity with open striplines case II-F. ($f = 0.817f_c^{TE_{10}}$, $\Delta h = 57.228 h$)	41
40	Field distribution for the cavity with open striplines case II-F. ($f = 1.144f_c^{TE_{10}}$, $\Delta h = 57.228 h$)	42
41	Field distribution for the cavity with open striplines case II-F. ($f = 1.144f_c^{TE_{10}}$, $\Delta h = 6.716 h$)	43
42	Schematic diagram of the cavity with bended striplines case II-G.	44
43	Top view of the cavity with bended striplines case II-G at $h = 0.25mm$	45
44	Computed S-parameters for the cavity with bended striplines case II-G.	46
45	Computed S-parameters for the cavity with bended striplines case II-G.	46
46	Field Distribution for the cavity with bended striplines case II-G. ($f = 0.768f_c^{TE_{10}}$, $\Delta h = 56.76 h$)	47
47	Field Distribution for the cavity with bended striplines case II-G. ($f = 1.44f_c^{TE_{10}}$, $\Delta h = 56.76 h$)	48
48	Field Distribution for the cavity with bended striplines case II-G. ($f = 1.44f_c^{TE_{10}}$, $\Delta h = 6.2 h$)	49

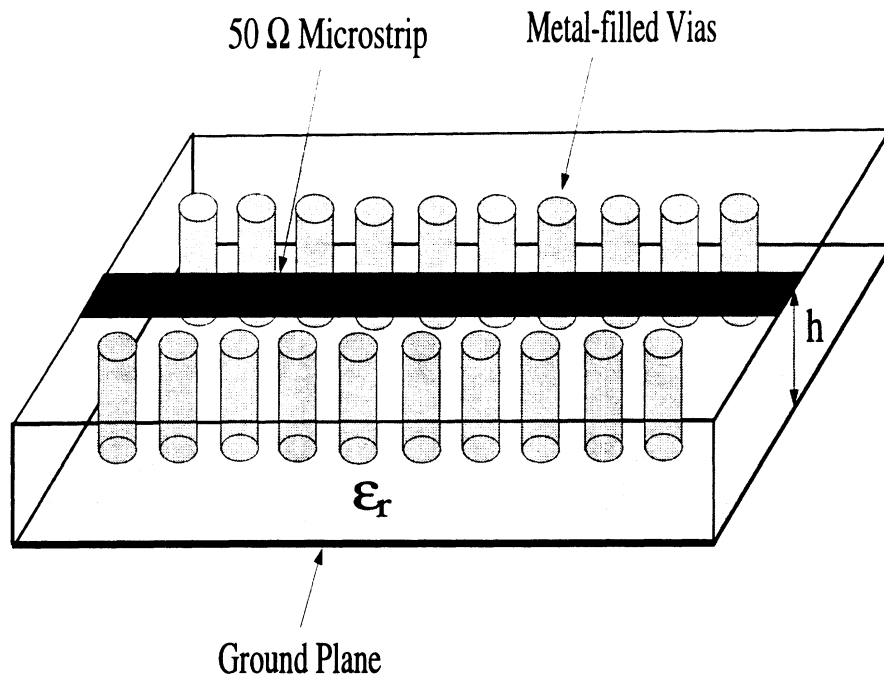


Figure 1: Schematic diagram of the microstrip case II-A.

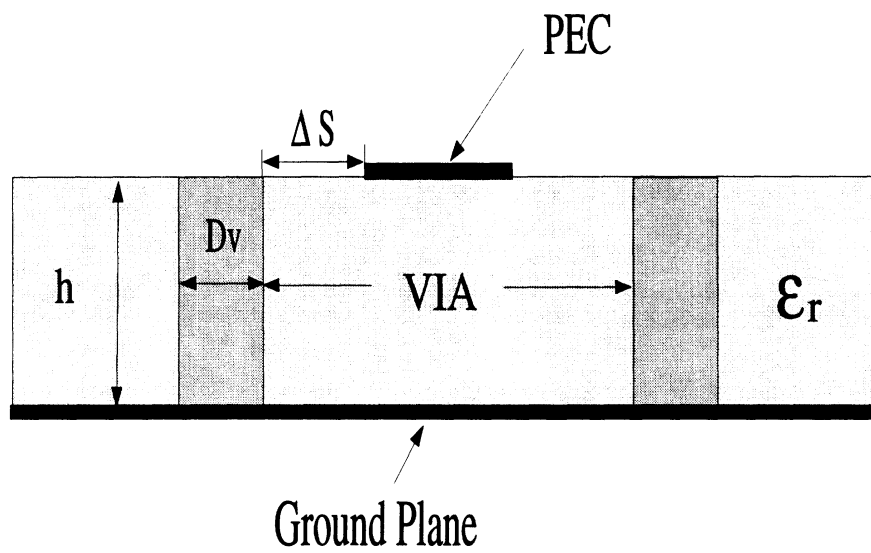


Figure 2: Cross section view of the microstrip case II-A.

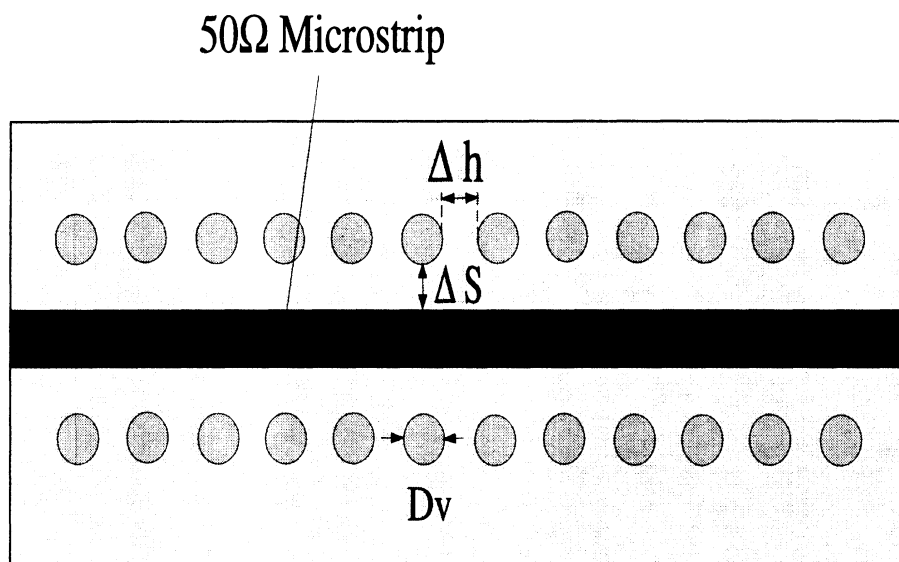


Figure 3: Top view of the microstrip case II-A.

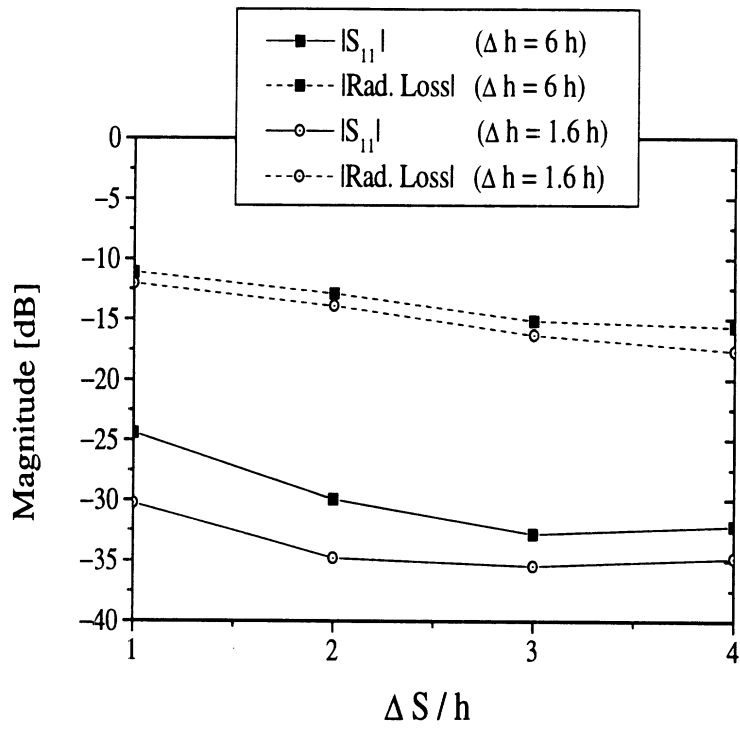


Figure 4: Computed return loss and rad. loss for the microstrip case II-A.

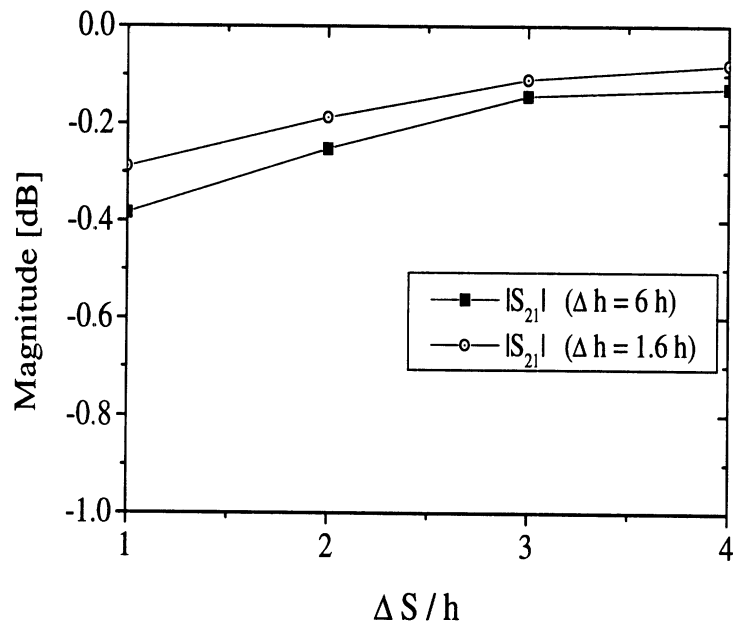


Figure 5: Computed insertion loss for the microstrip case II-A.

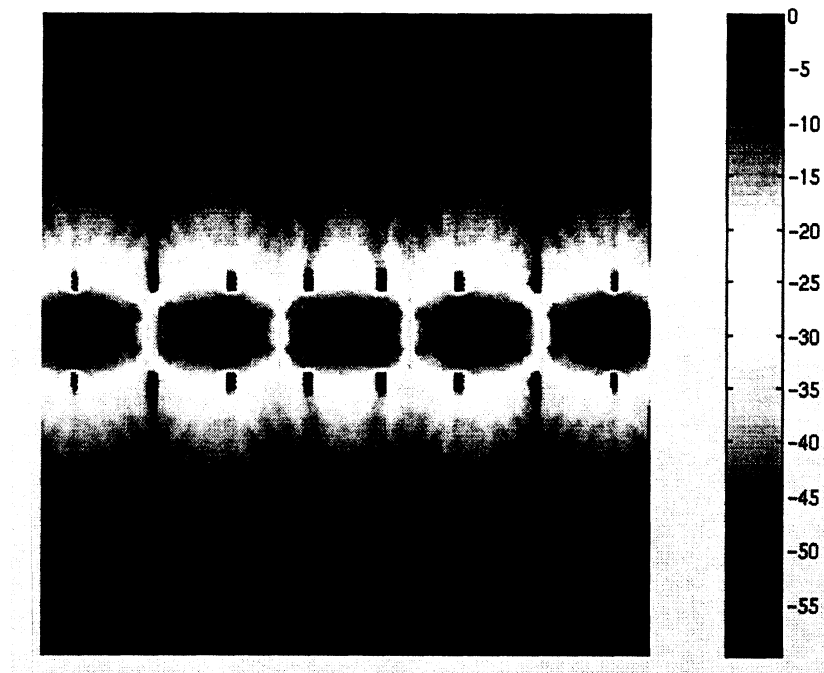


Figure 6: Field distribution for the microstrip case II-A at 25GHz ($\Delta h = 6$ h).

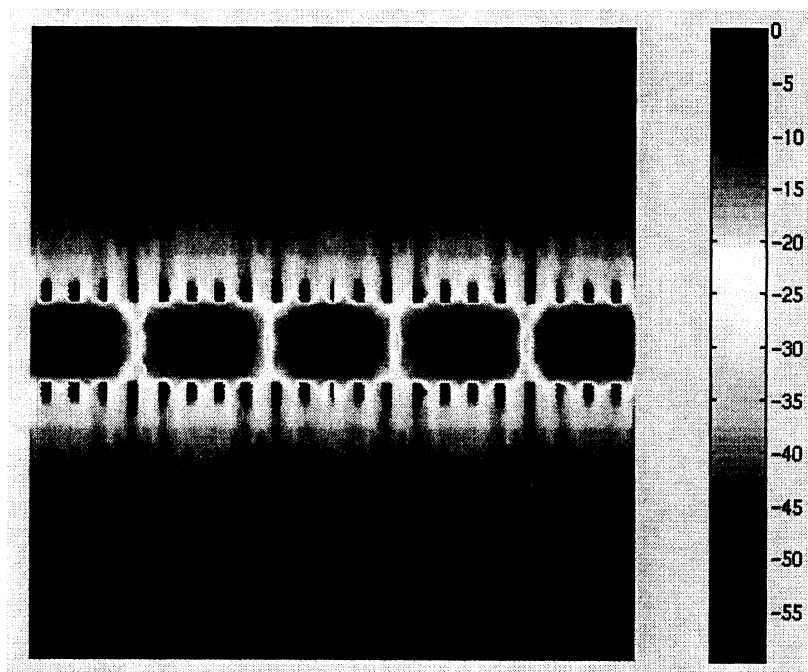


Figure 7: Field distribution for the microstrip case II-A at 25GHz ($\Delta h = 1.6$ h).

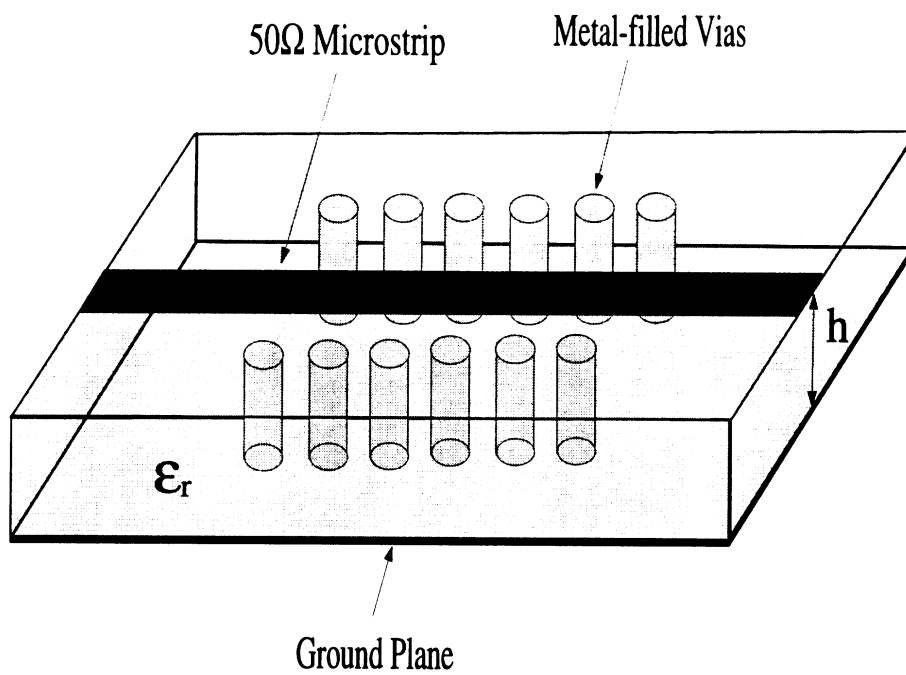


Figure 8: Schematic diagram of the microstrip case II-B.

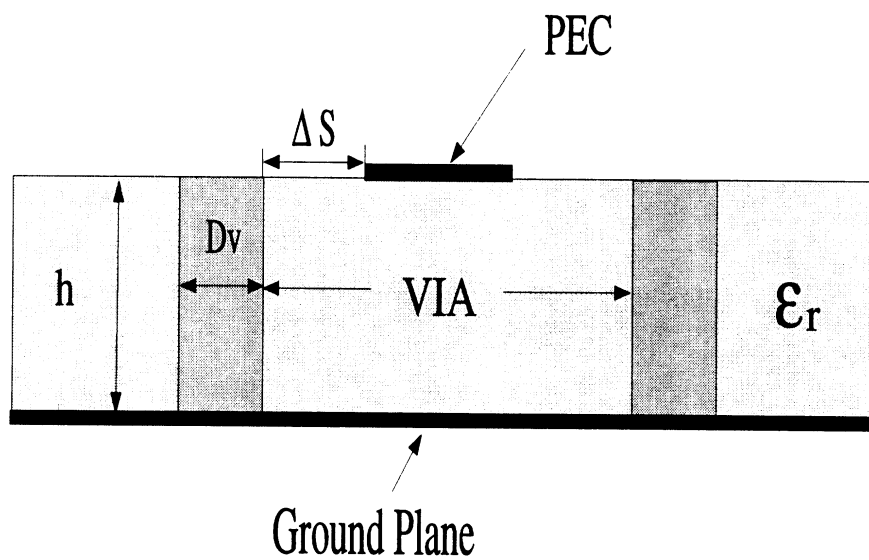


Figure 9: Cross section view of the microstrip case II-B.

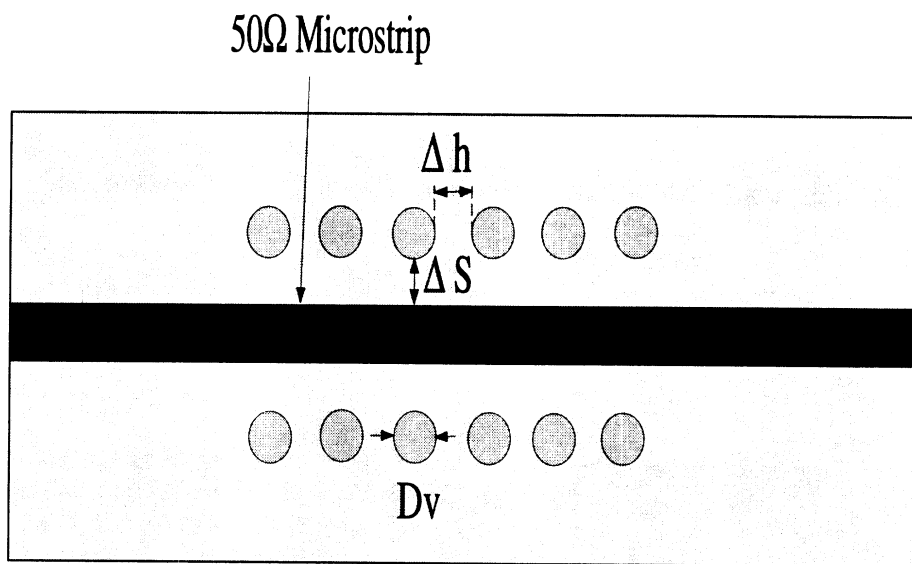


Figure 10: Top view of the microstrip case II-B.

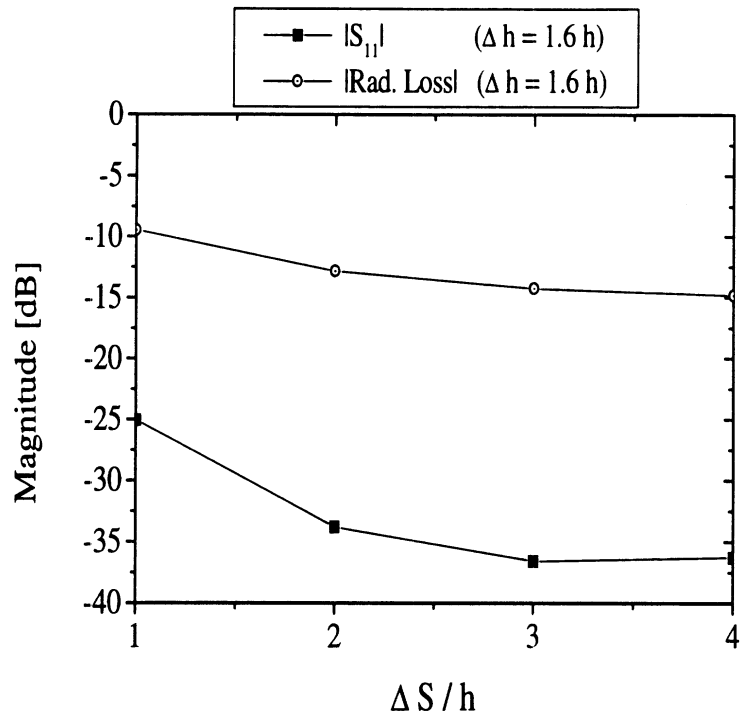


Figure 11: Computed return loss and rad. loss for the microstrip case II-B.

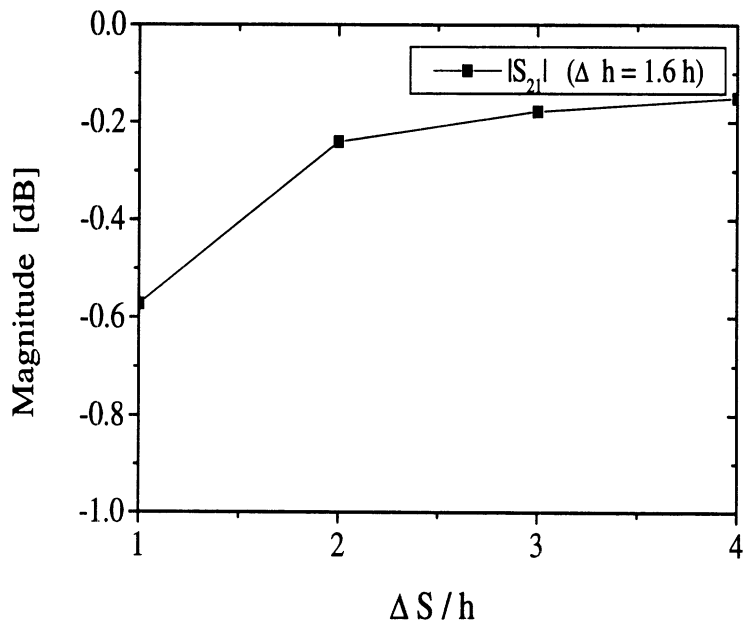


Figure 12: Computed insertion loss for the microstrip case II-B.

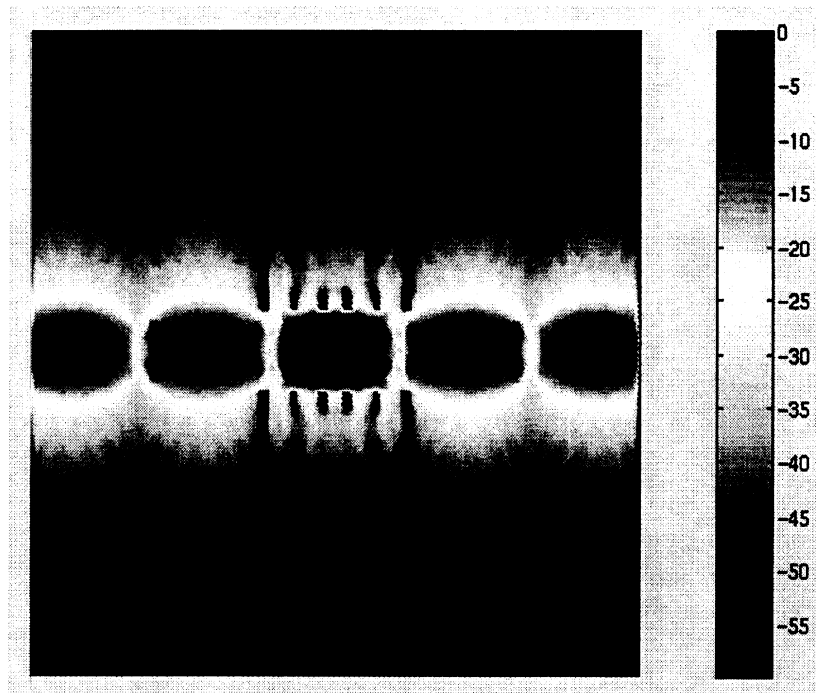


Figure 13: Field distribution for the microstrip case II-A at 25GHz ($\Delta h = 1.6 h$).

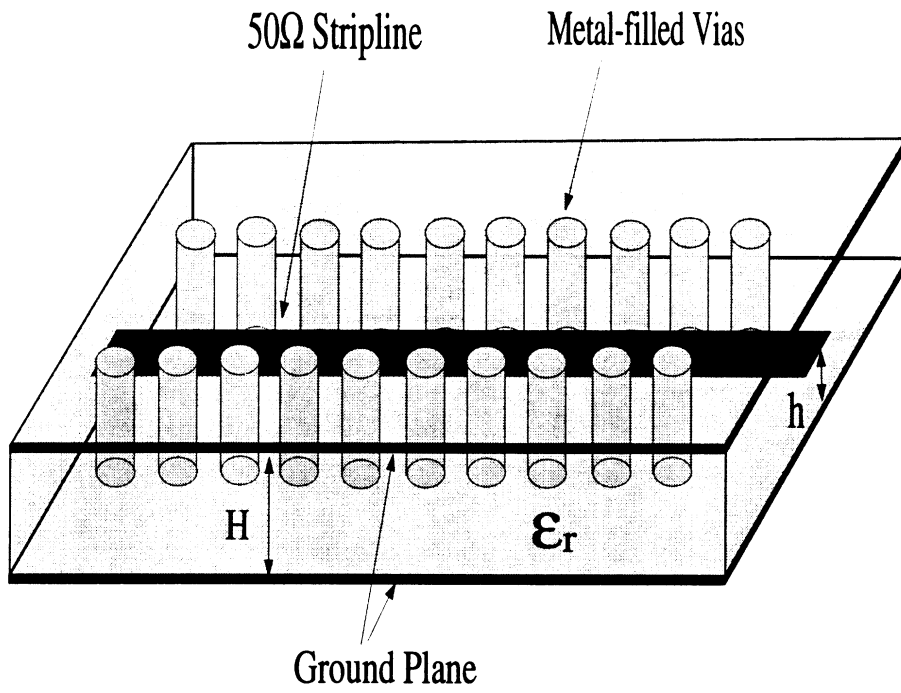


Figure 14: Schematic diagram of the stripline case II-C.

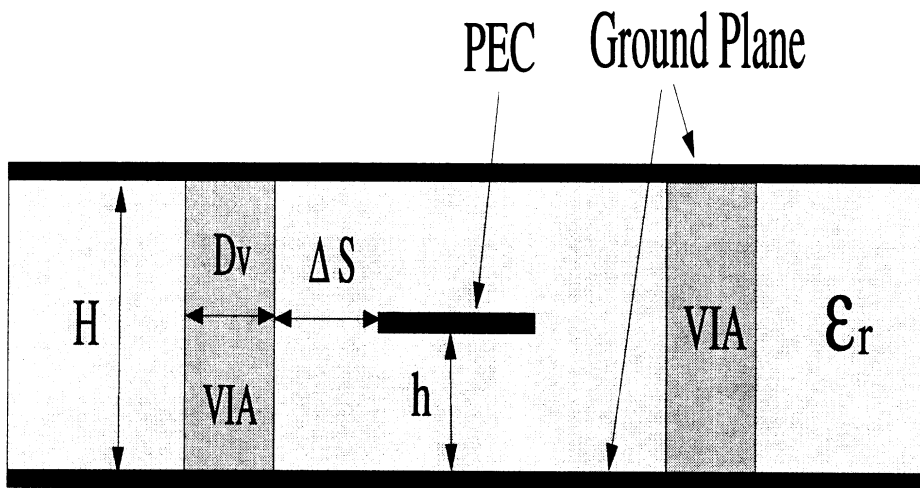


Figure 15: Cross section view of the stripline case II-C.

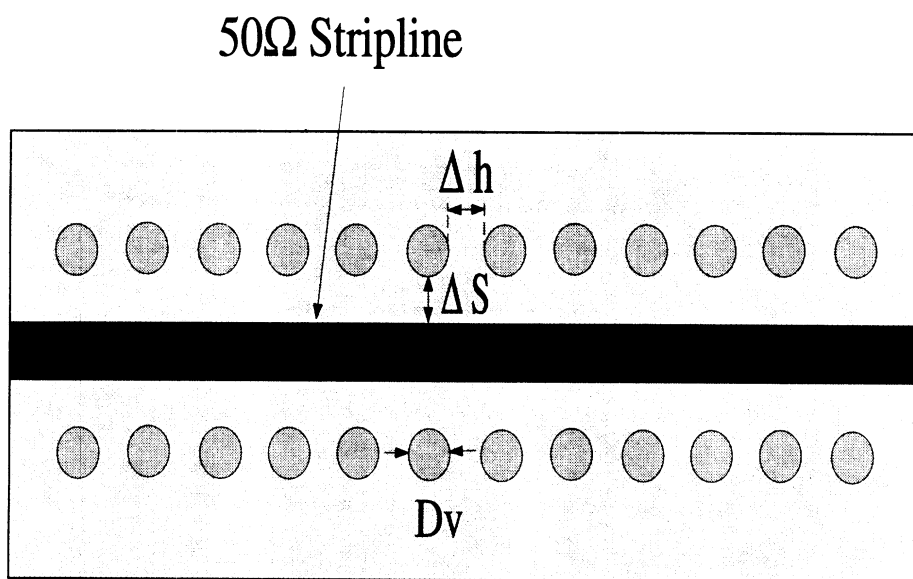


Figure 16: Top view of the stripline case II-C at $h = 0.25mm$.

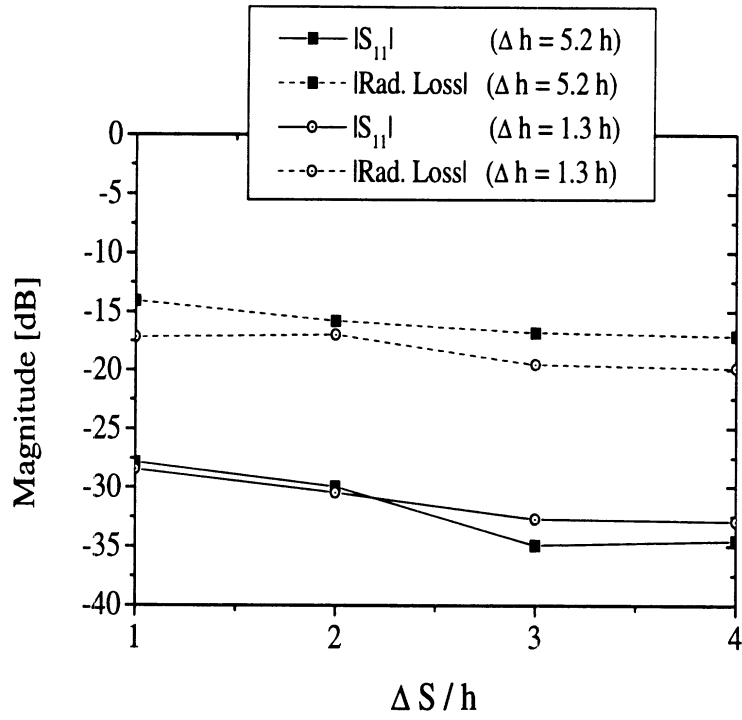


Figure 17: Computed return loss and rad. loss for the stripline case II-C.

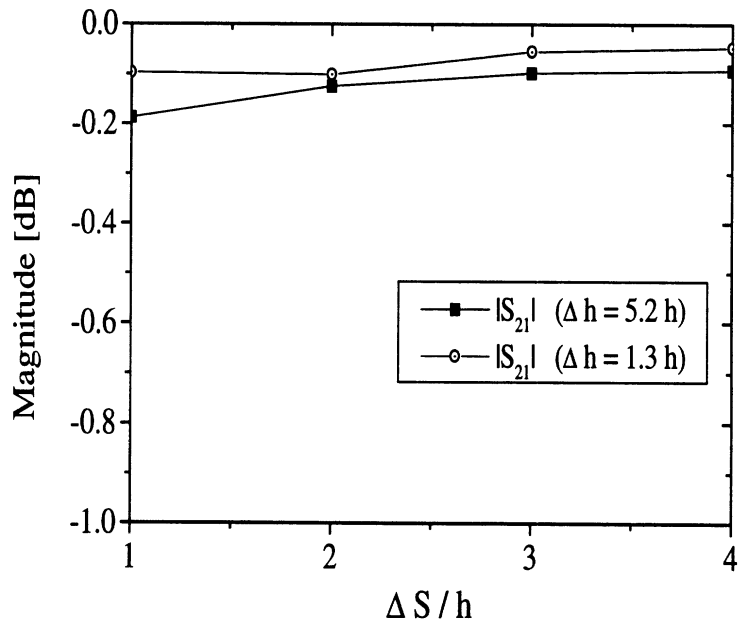


Figure 18: Computed insertion loss for the stripline case II-C.

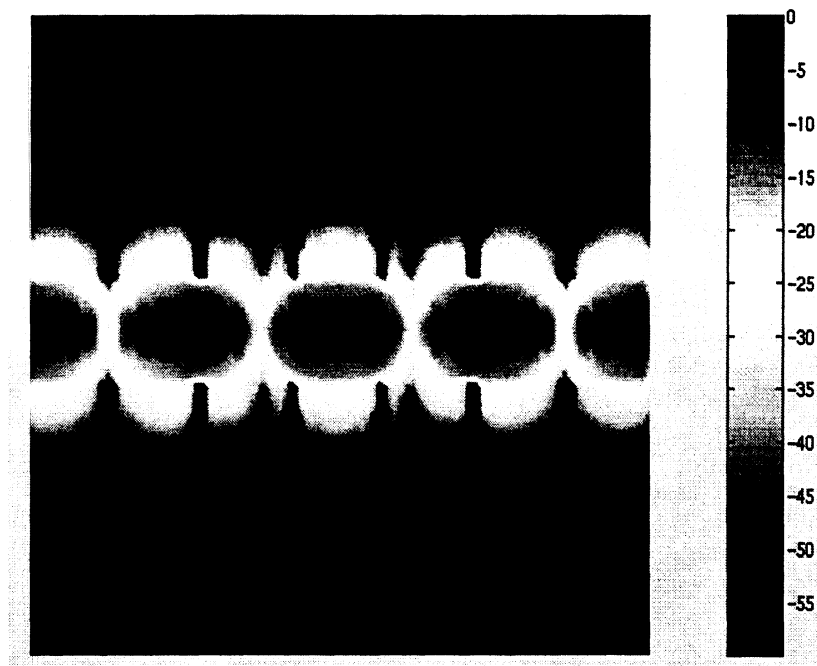


Figure 19: Field distribution of the stripline case II-C at 25GHz. ($\Delta h = 5.2 h$)

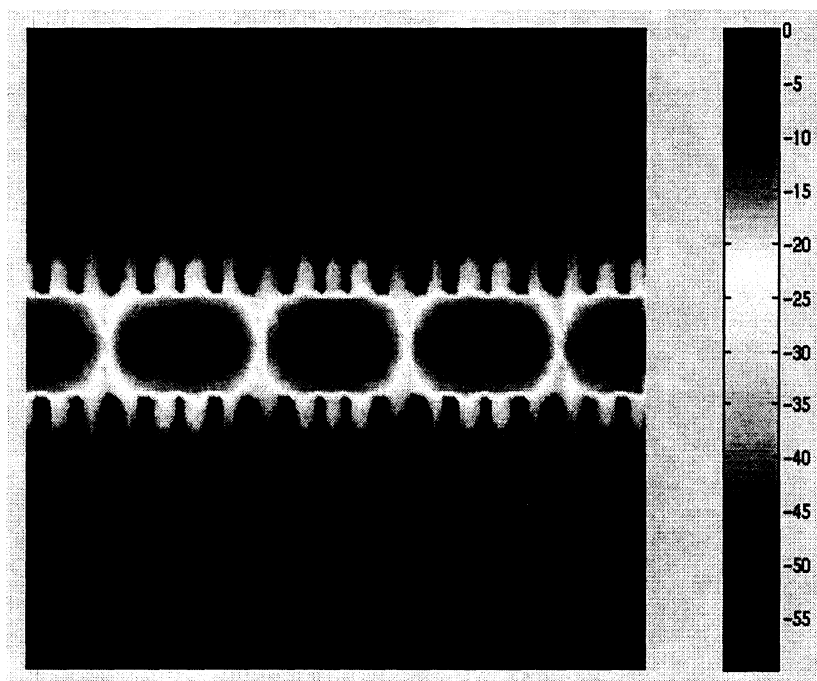


Figure 20: Field distribution of the stripline case II-C at 25GHz. ($\Delta h = 1.3 h$)

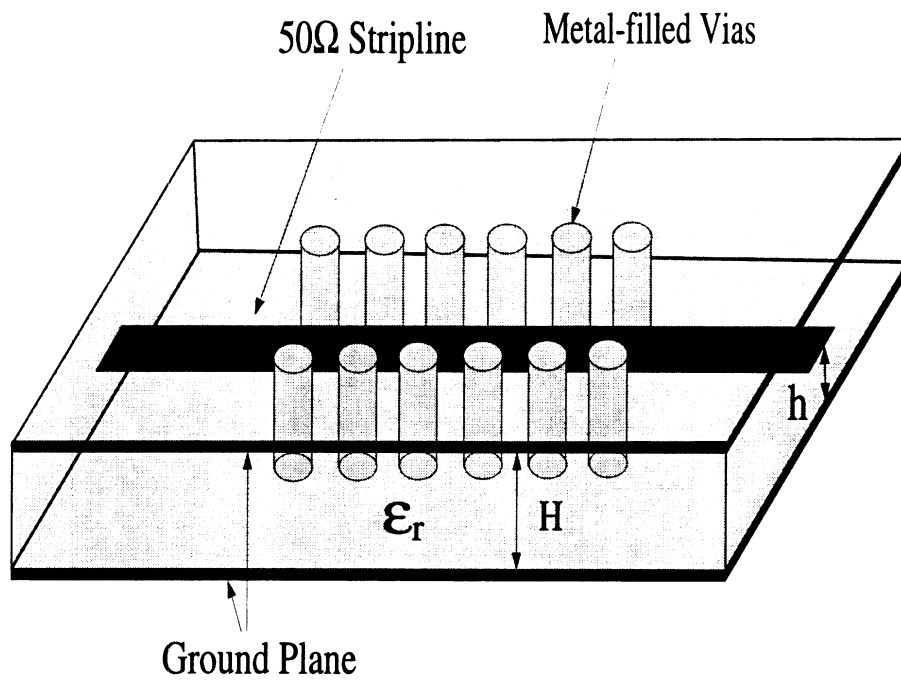


Figure 21: Schematic diagram of the stripline case II-D.

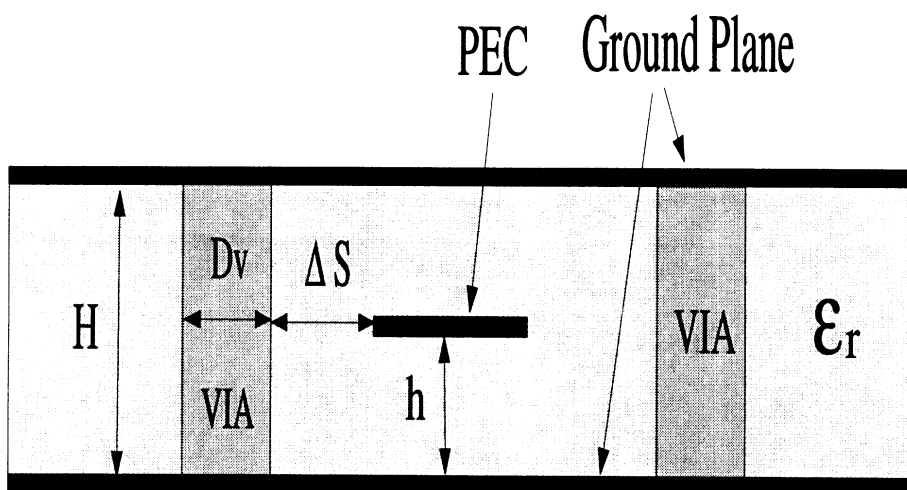


Figure 22: Cross section view of the stripline case II-D.

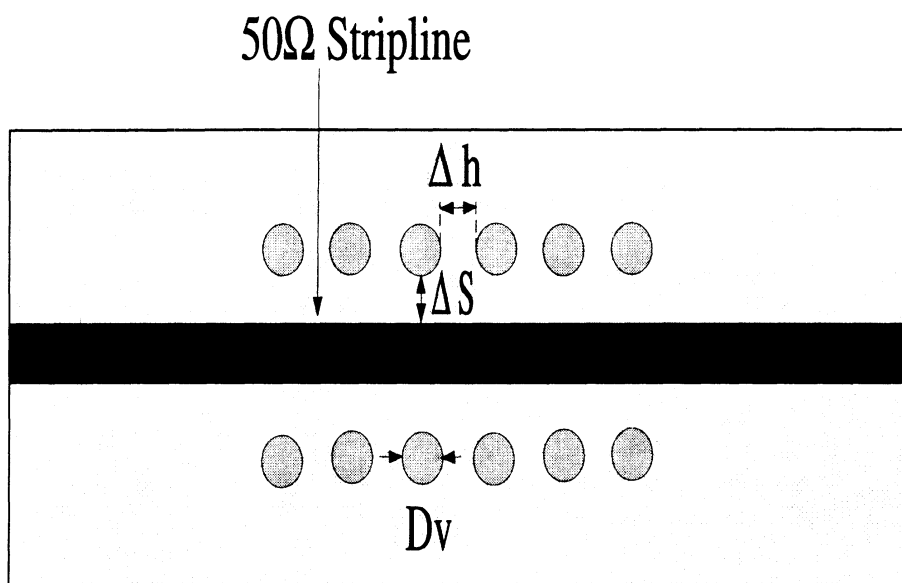


Figure 23: Top view of the stripline case II-D at $h = 0.25mm$.

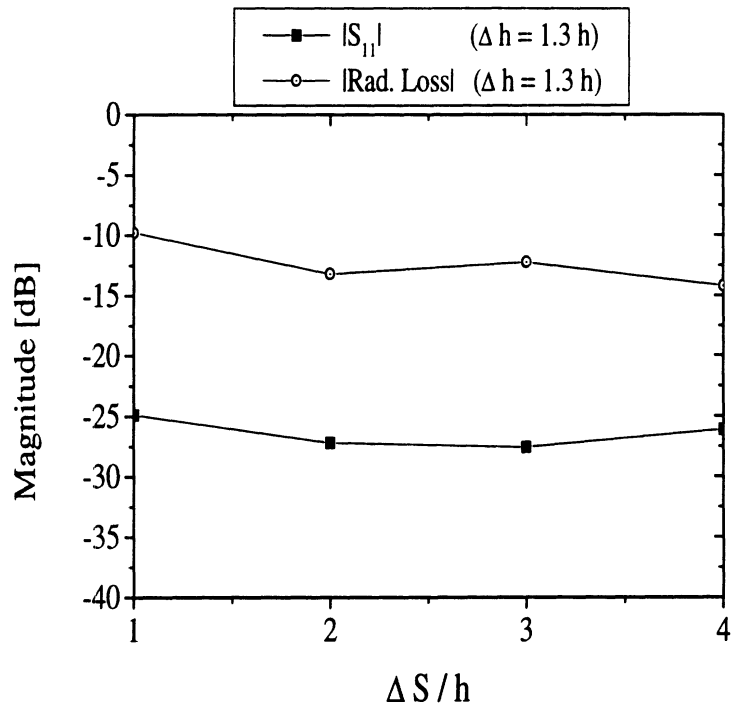


Figure 24: Computed return loss and rad. loss for the stripline case II-D.

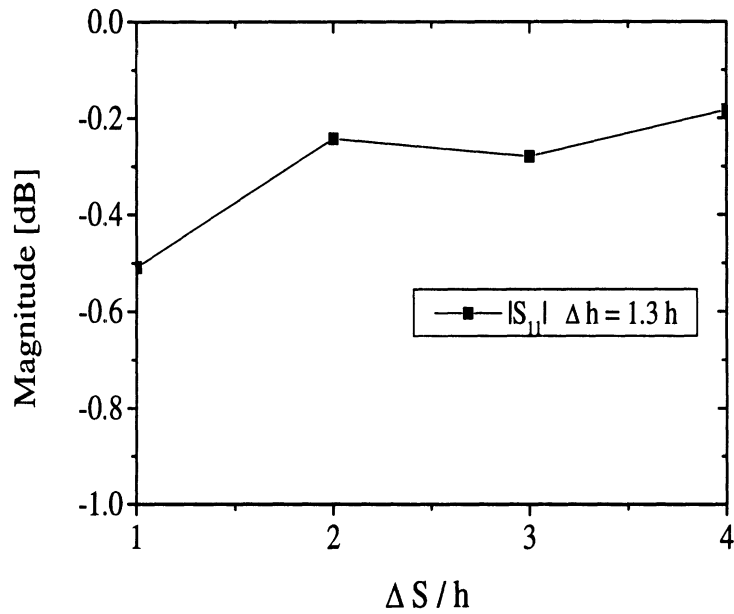


Figure 25: Computed insertion loss for the stripline case II-D.

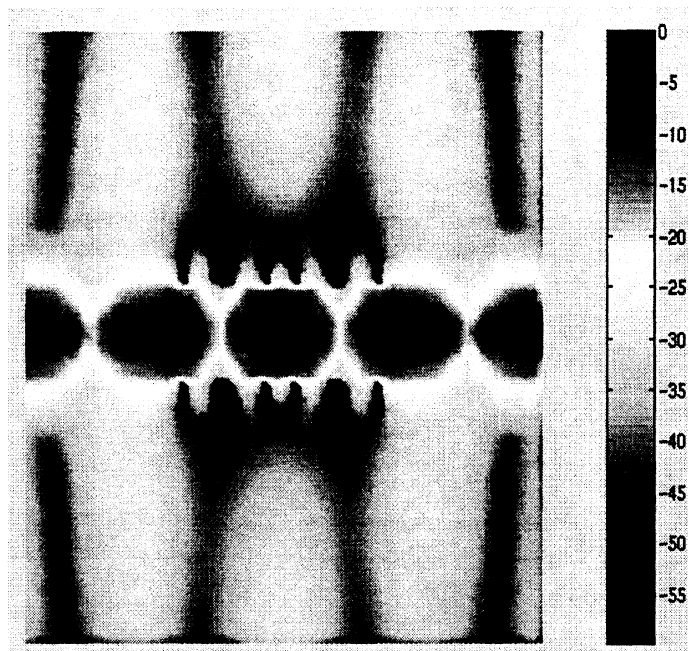


Figure 26: Field distribution of the stripline case II-D at 35GHz. ($\Delta h = 1.3 h$)

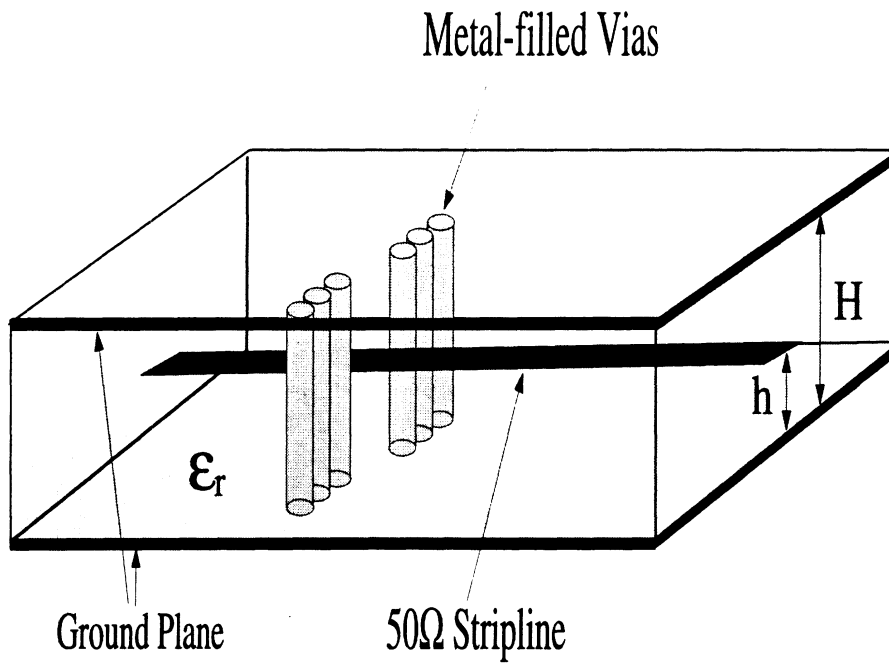


Figure 27: Schematic diagram of the stripline case II-E.

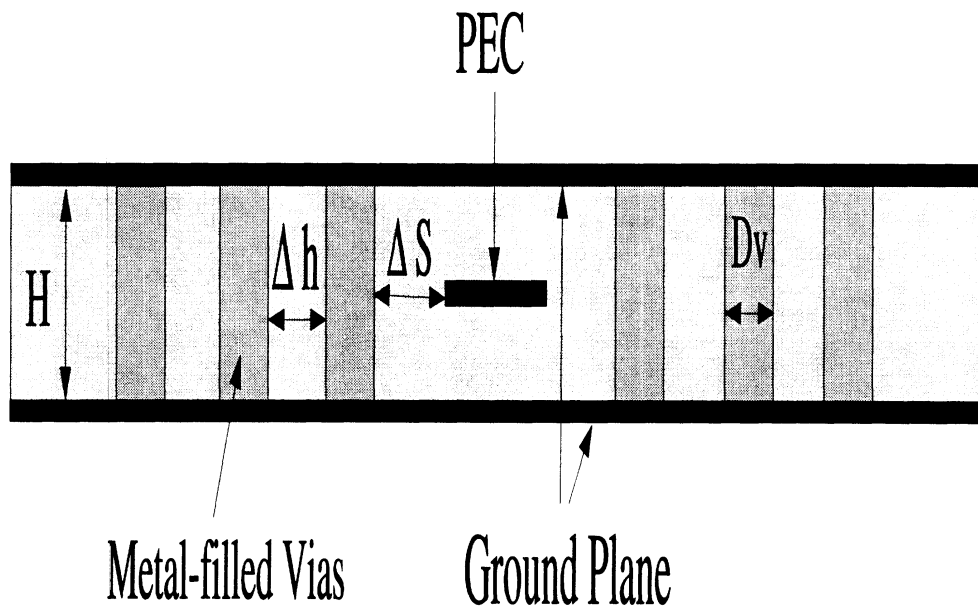


Figure 28: Cross section view the stripline case II-E.

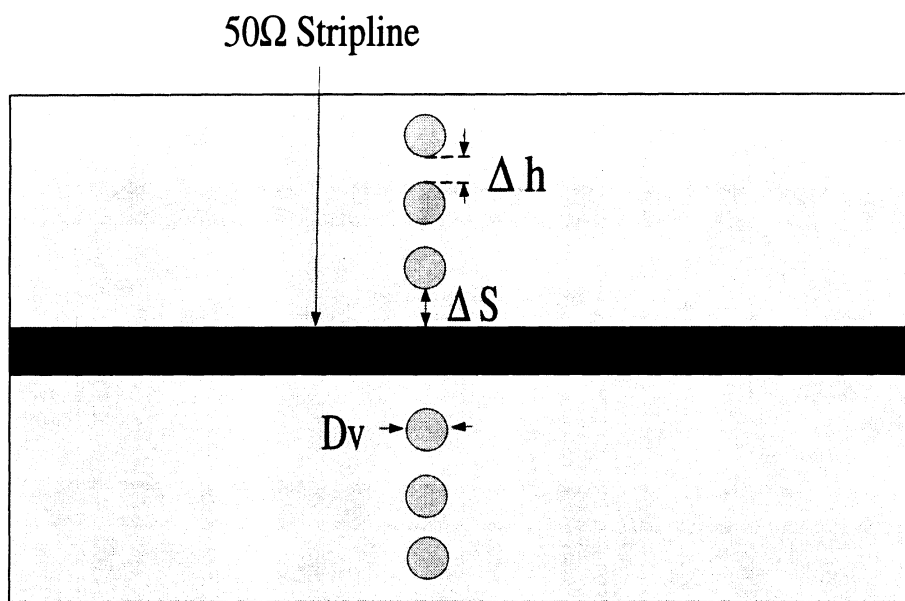


Figure 29: Top view of the stripline case II-E at $h = 0.25mm$.

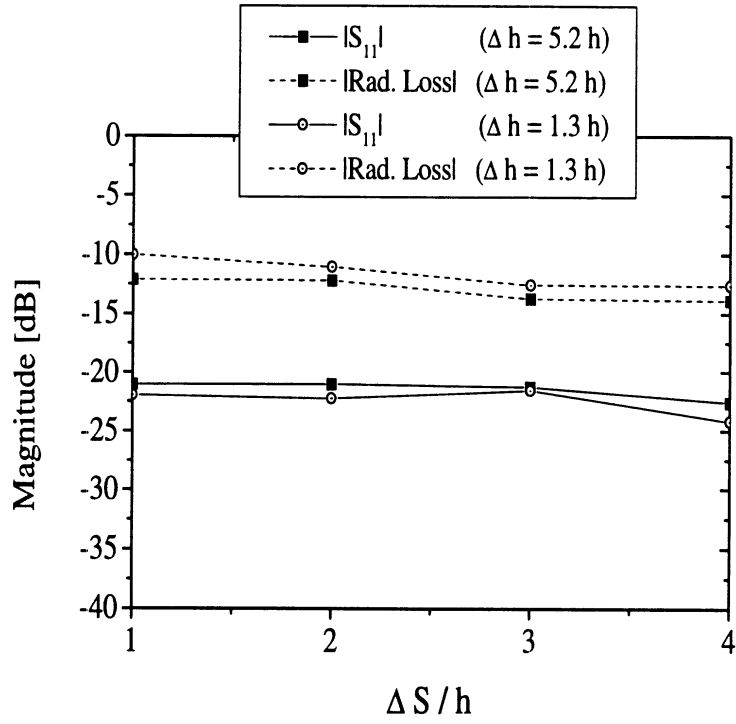


Figure 30: Computed return loss and rad. loss for the stripline case II-E.

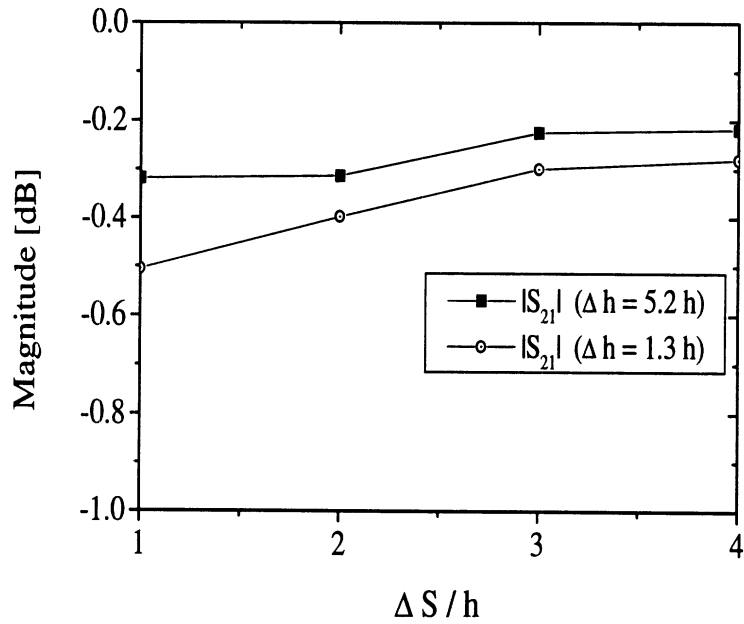


Figure 31: Computed insertion loss for the stripline case II-E.

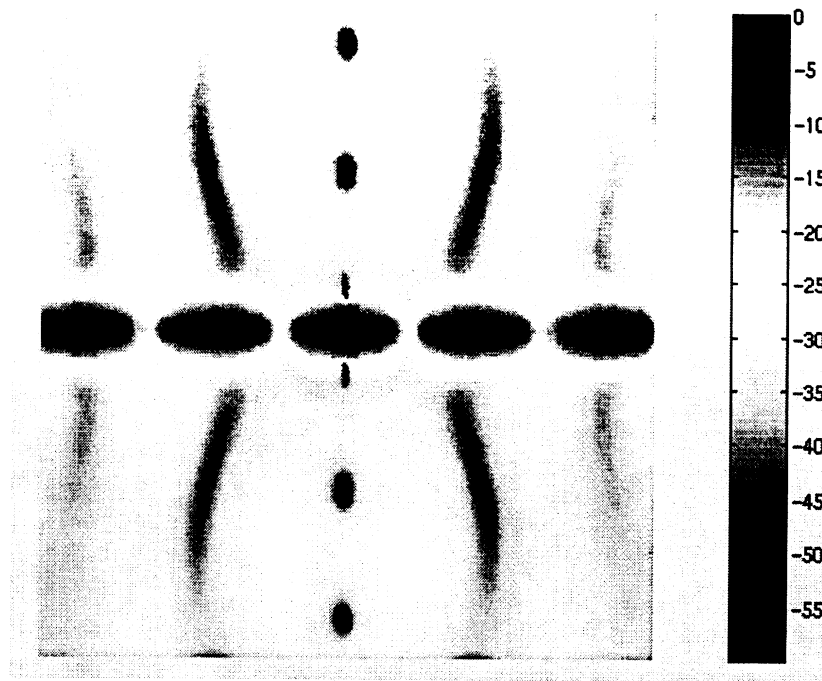


Figure 32: Field distribution of the stripline case II-E at 28GHz. ($\Delta h = 5.2$ h)

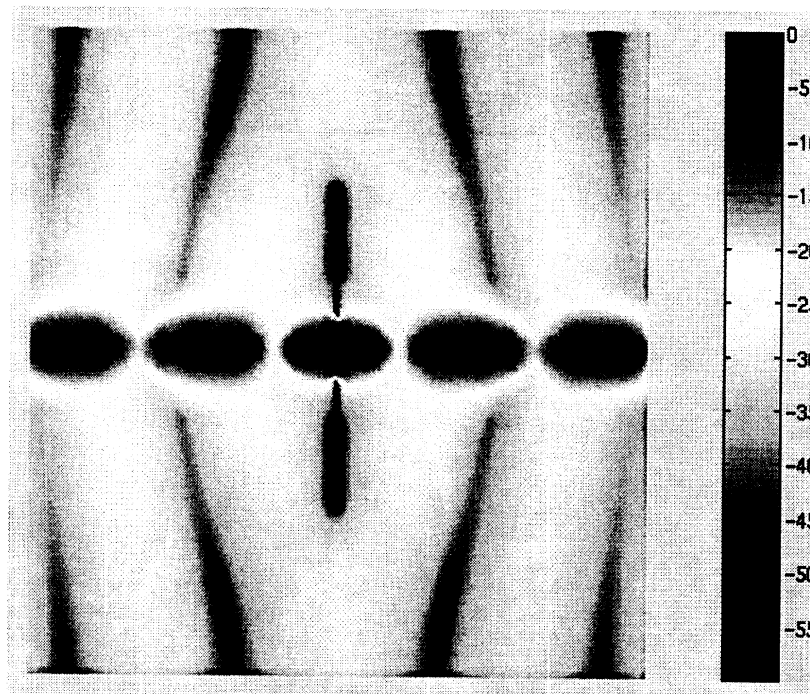


Figure 33: Field distribution of the stripline case II-E at 28GHz. ($\Delta h = 1.3$ h)

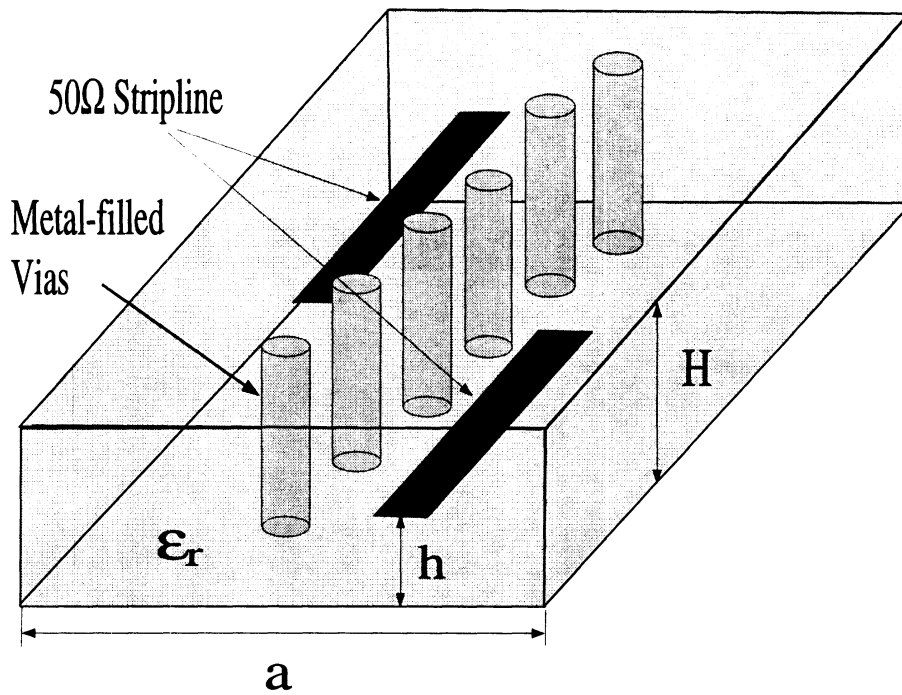


Figure 34: Schematic diagram of the cavity with open striplines case II-F.

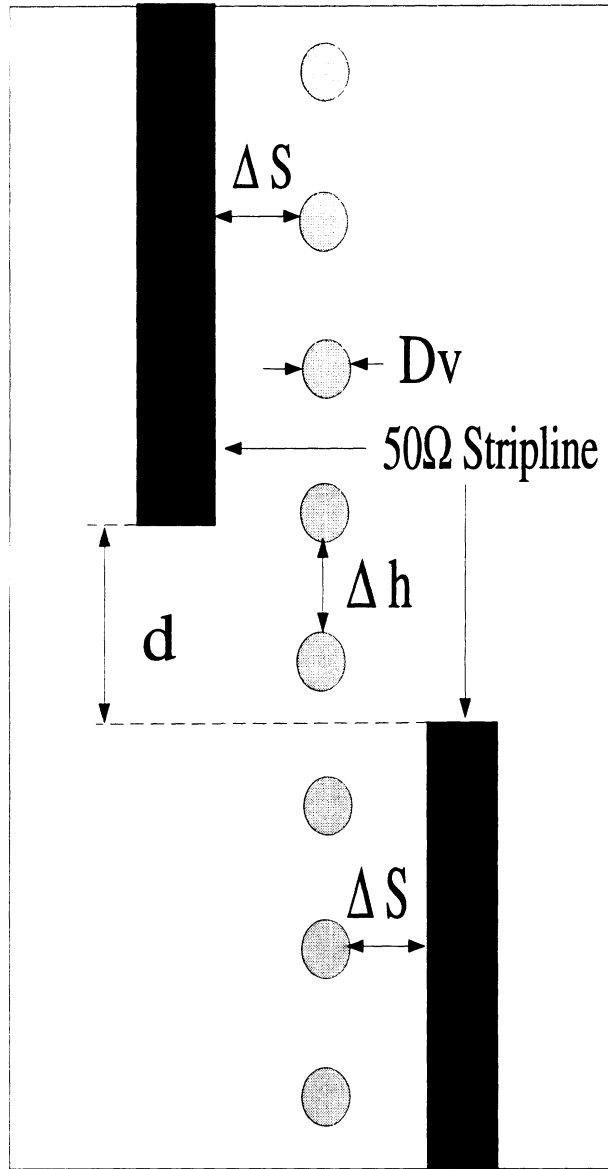


Figure 35: Top view of the cavity with open striplines case II-F at $h = 0.25mm$.

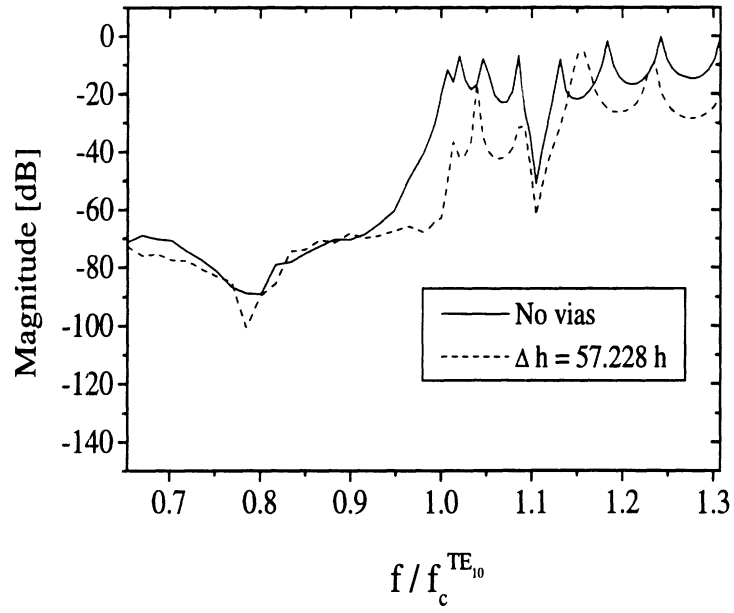


Figure 36: Ratio of maximum field value for the cavity with open striplines case II-F.

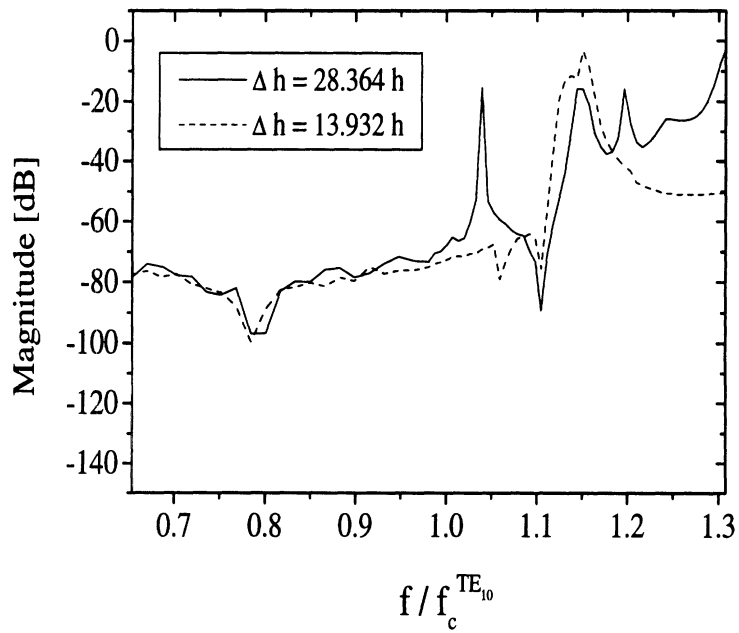


Figure 37: Ratio of maximum field value for the cavity with open striplines case II-F.

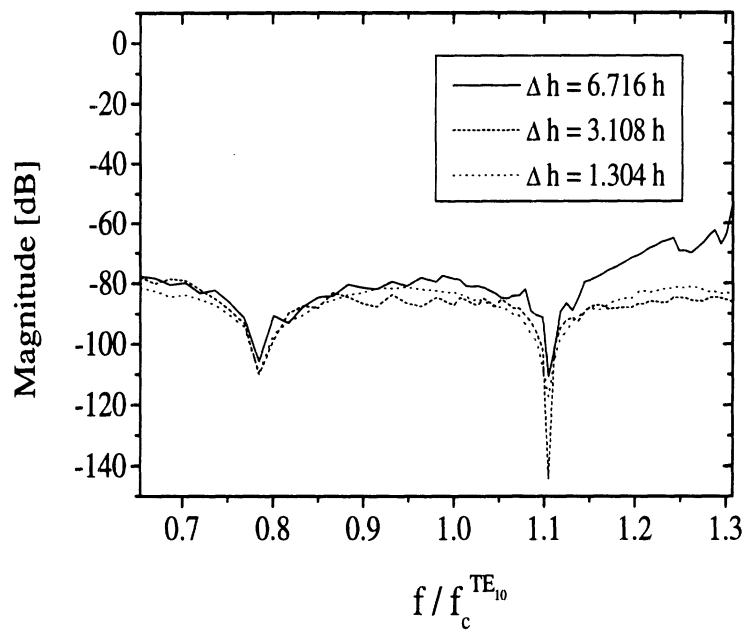


Figure 38: Ratio of maximum field value for the cavity with open striplines case II-F.

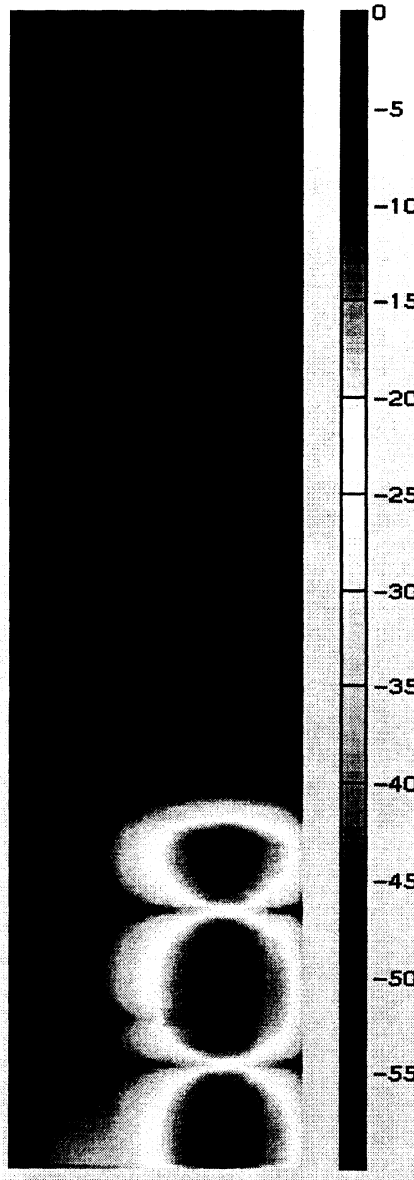


Figure 39: Field distribution for the cavity with open striplines case II-F. ($f = 0.817f_c^{TE_{10}}$, $\Delta h = 57.228 h$)

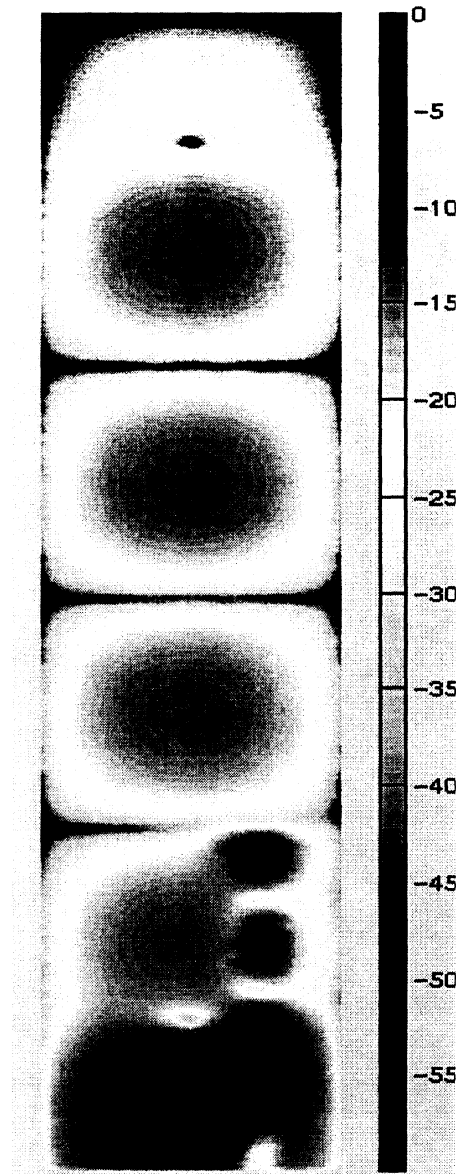


Figure 40: Field distribution for the cavity with open striplines case II-F. ($f = 1.144 f_c^{TE_{10}}$, $\Delta h = 57.228 h$)

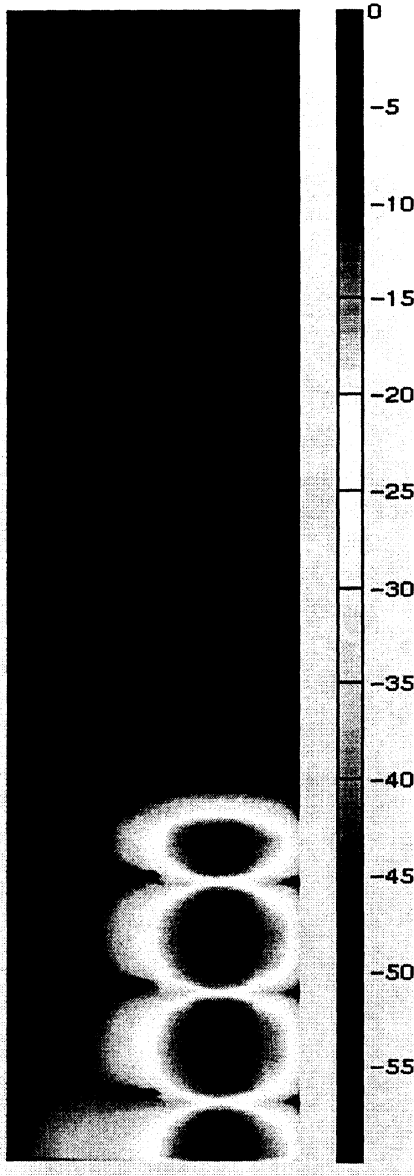


Figure 41: Field distribution for the cavity with open striplines case II-F. ($f = 1.144 f_c^{TE_{10}}$, $\Delta h = 6.716 h$)

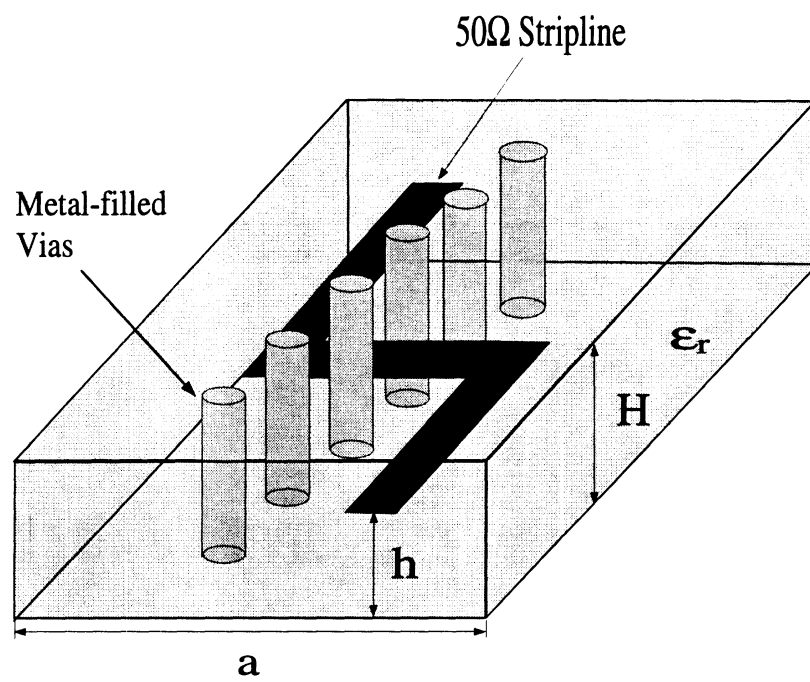


Figure 42: Schematic diagram of the cavity with bended striplines case II-G.

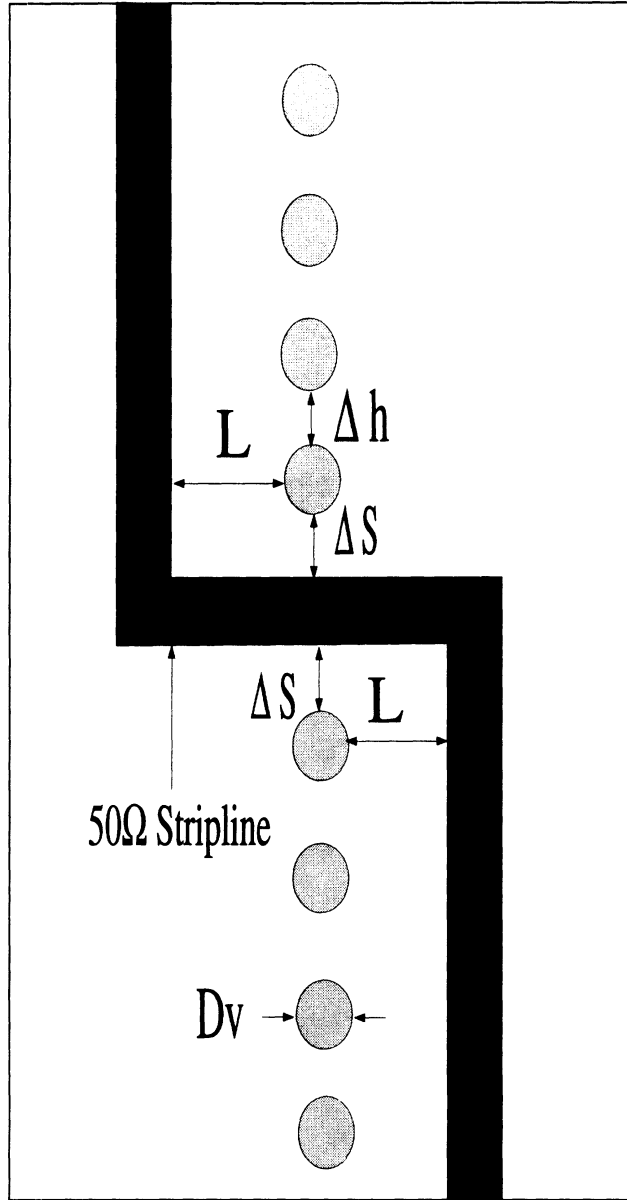


Figure 43: Top view of the cavity with bended striplines case II-G at $h = 0.25mm$.

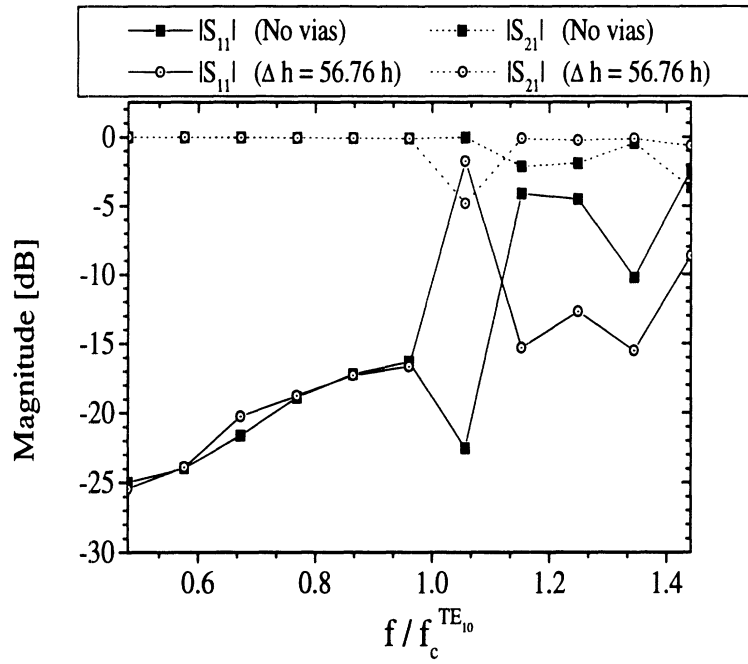


Figure 44: Computed S-parameters for the cavity with bended striplines case II-G.

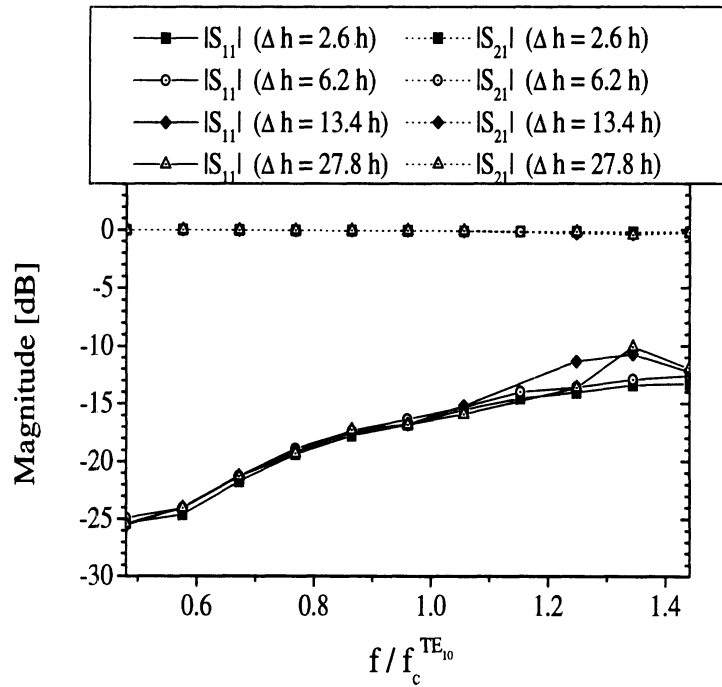


Figure 45: Computed S-parameters for the cavity with bended striplines case II-G.

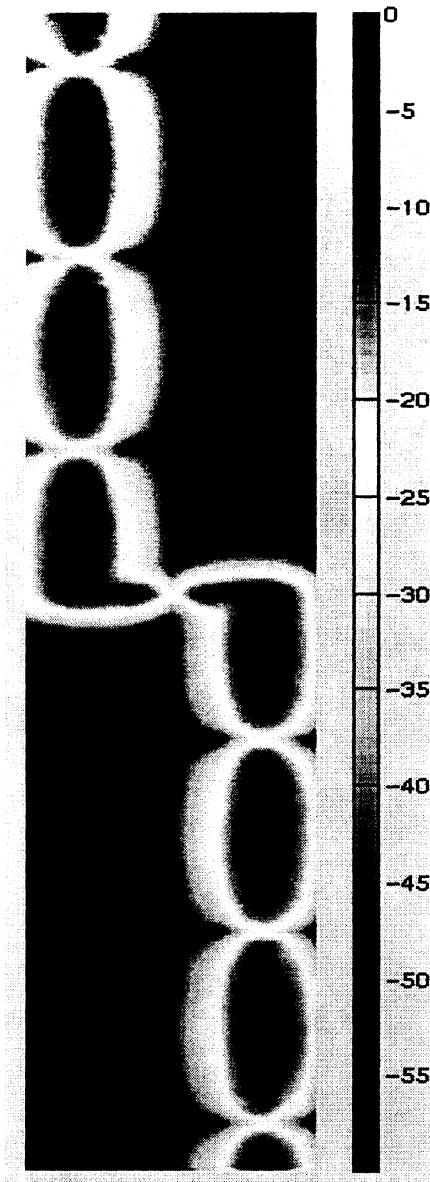


Figure 46: Field Distribution for the cavity with bended striplines case II-G. ($f = 0.768 f_c^{TE_{10}}$, $\Delta h = 56.76 \text{ h}$)



Figure 47: Field Distribution for the cavity with bended striplines case II-G. ($f = 1.44f_c^{TE_{10}}$, $\Delta h = 56.76 h$)

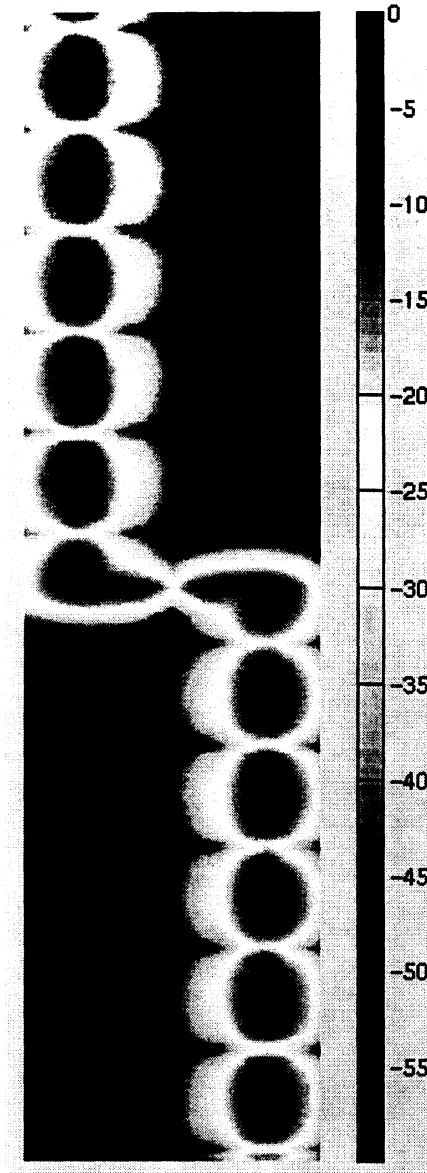


Figure 48: Field Distribution for the cavity with bended striplines case II-G. ($f = 1.44f_c^{TE_{10}}$, $\Delta h = 6.2 h$)